UHASSELT
KNOWLEDGE IN ACTION

Maastricht University

Faculty of Medicine and Life Sciences
School for Life Sciences
Master of Biomedical Sciences

Master's thesis

Unravelling Redox-Mediated Tissue Regeneration in Schmidtea mediterranea: The Role of Riboflavin (Vitamin B2) and the Keap1/Nrf2 Pathway

Renée Rita Moonen

Thesis presented in fulfillment of the requirements for the degree of Master of Biomedical Sciences, specialization Molecular Mechanisms in Health and Disease

SUPERVISOR :

Prof. dr. Karen SMEETS

MENTOR :

De heer Martijn HELEVEN

2023
2024

Transnational University Limburg is a unique collaboration of two universities in two countries: the University of Hasselt and Maastricht University.

UHASSELT
KNOWLEDGE IN ACTION

www.uhasselt.be
Universiteit Hasselt
Campus Hasselt:
Martelarenlaan 42 | 3500 Hasselt
Campus Diepenbeek:
Agoralaan Gebouw D | 3590 Diepenbeek

UHASSELT
KNOWLEDGE IN ACTION

Maastricht University

Faculty of Medicine and Life Sciences
School for Life Sciences
Master of Biomedical Sciences

Master's thesis

Unravelling Redox-Mediated Tissue Regeneration in Schmidtea mediterranea: The Role of Riboflavin (Vitamin B2) and the Keap1/Nrf2 Pathway

Renée Rita Moonen

Thesis presented in fulfillment of the requirements for the degree of Master of Biomedical Sciences, specialization Molecular Mechanisms in Health and Disease

SUPERVISOR :

Prof. dr. Karen SMEETS

MENTOR :

De heer Martijn HELEVEN

Unravelling Redox-Mediated Regeneration in *Schmidtea mediterranea*: The Role of Riboflavin (Vitamin B_2) and the Keap1/Nrf2 Pathway *

Renée M.[1], Martijn H.[1], and Karen S.[1,2]

[1]Centre for Environmental Sciences, Hasselt University, Diepenbeek, Belgium
[2]Department of Biology and Geology, Faculty of Sciences, Agoralaan Building D, 3590, Diepenbeek, Belgium

*Running title: *Redox-Sensitive Compounds in Planarian Regeneration*

To whom correspondence should be addressed: Karen Smeets, Tel: +32 11 26 83 19; Email: karen.smeets@uhasselt.be

Keywords: *Schmidtea mediterranea*, regeneration, riboflavin, Keap1, SKN-1

ABSTRACT

Regeneration, the ability to restore lost or damaged tissues, is a complex and tightly regulated process of enduring scientific interest. The freshwater planarian *Schmidtea mediterranea*, known for its exceptional regenerative capacity, offers an invaluable model for investigating tissue repair. While the significance of the redox balance for successful regeneration has been established, the involvement of various redox-sensitive and redox-regulating molecules remains unclear. This research addresses these knowledge gaps by investigating the functional role of the redox-sensitive molecule, riboflavin and the redox-regulating Keap1/Nrf2 pathway during planarian regeneration. To investigate this, RNAi was employed to silence genes related to riboflavin metabolism and transport, as well as genes related to the Keap1/Nrf2 pathway. Following knockdown of riboflavin-related targets, blastema and photoreceptor (eye) formation, stem cell proliferation, and neurodevelopment were studied, along with the expression patterns of the riboflavin transporter during regeneration. The impact of Keap1 and SKN-1 knockdown on blastema and eye formation, and neurodevelopment was assessed in addition to the effects of gene silencing under conditions of induced oxidative stress. Our data reveal that riboflavin metabolism is essential for successful tissue regeneration, photoreceptor development, and dopaminergic neuron development. Additionally, riboflavin transport appears important for stem cell proliferation and maintaining riboflavin availability in the planarian body. Furthermore, our study confirms the presence of Keap1 and SKN-1 in *S. mediterranea* with a redox-regulating role during regeneration. Collectively, these findings addresses research gaps in the current understanding of redox-mediated planarian regeneration and offer valuable insights into biological processes relevant to the advancement of regenerative medicine.

INTRODUCTION

The regeneration process - Regeneration, the remarkable ability of certain organisms to restore lost or damaged tissues, has fascinated scientists for centuries. This biological phenomenon allows for reestablishing the tissue's natural morphology and functional integrity without scar tissue formation (1-3). At the cellular level, this includes cell proliferation, migration, and differentiation, all under precise genetic and molecular control (3). Despite distinct common features, such as cellular plasticity, stem cell populations, and shared signalling pathways, regenerative capacity and processes vary widely across the different taxa within the animal kingdom (1, 2, 4). Mammals, for instance, generally exhibit constrained regenerative abilities. This is exemplified by humans, displaying limited regenerative potential in hepatic and dermal tissues, and mice, showcasing the capacity for digit tip regeneration amid otherwise restricted regenerative capacities (1, 5, 6). However, some organisms exhibit impressive regenerative abilities. These abilities can range from limb regeneration observed in salamanders (e.g., axolotl) and starfish to heart regeneration in zebrafish, and even full-body regeneration from small tissue fragments in invertebrates such as Hydra and planarians (1, 3, 6-8). Given the limited regenerative capacity of the most

commonly used animal models in biomedical research, such as mice, researchers turn to highly regenerative animals as invaluable models for studying the intricate cellular and molecular mechanisms underpinning tissue repair. In light of these remarkable capabilities, such organisms offer unparalleled opportunities to expand our understanding of regeneration (3, 9).

Schmidtea mediterranea (*S. mediterranea*), a freshwater planarian native to the Mediterranean region, has emerged as a prominent model organism for studying regeneration due to several attractive features: (1) approximately 30% of their total cell population is constituted by neoblasts, a population of adult pluripotent stem cells (PSCs), with characteristic embryonic-like cell properties, which allow for (2) the extraordinary capacity to regenerate a complete functional body from small tissue fragments in only 7-14 days, including the remarkable ability to regenerate their central nervous system (CNS), and finally, (3) these planarians use evolutionary conserved signalling pathways to orchestrate cell differentiation, patterning and morphogenesis (1-3, 10). Moreover, *S. mediterranea* offers several experimental advantages, such as ease of maintenance, a relatively simple anatomy, and the absence of ethical considerations typically associated with vertebrate models. In this study, the asexual strain of *S. mediterranea* is used, which reproduces solely by transverse bisection (binary fission) into two pieces (11).

Tissue regeneration in *S. mediterranea* is a tightly regulated process, necessitating the precise coordination of numerous molecular, cellular, and physiological events. Planarian regeneration is typically initiated upon detection of amputation or injury, prompting a rapid response from cells adjacent to the lesion. These early injury signals trigger a cascade of cellular responses to initiate wound healing (12-14). This process involves the rapid migration of adjacent epithelial cells to facilitate wound closure, complemented by the migration of neoblasts to the injury site. Neoblasts, which harbour the capacity for self-renewal and can differentiate into all cell types found in the body, serve as the primary drivers of regeneration (14, 15). Once activated, they proliferate, generating a pool of progenitor cells at the wound site. This results in the formation of an undifferentiated and unpigmented cell mass known as the blastema, which serves as the epicentre for tissue regeneration. Here, intricate processes of differentiation, patterning, and morphogenesis take place to eventually replace the lost or damaged body structure. As aforementioned, these processes are tightly regulated by a network of highly conserved signalling pathways, including the Hedgehog, Wnt/β-catenin, BMP, and EGFR pathways, to ensure successful tissue regeneration (3, 12-14). Among these evolutionary conserved pathways, the significant mitogen-activated protein kinase (MAPK)/extracellular signal-regulated kinase (ERK) pathway emerges as a central regulator of cellular responses during regeneration. Upon activation, this signalling cascade triggers a series of intracellular events that ultimately regulate gene expression and orchestrate the cellular responses necessary for tissue regeneration, such as cell proliferation, differentiation, and morphogenesis (3, 16). Second messengers, including calcium (Ca^{2+}) and reactive oxygen species (ROS), were shown to be crucial in the activation process of these signalling pathways (13).

Reactive oxygen species – ROS, which include free radicals like superoxide radicals ($O_2^{\bullet-}$) and non-radicals like hydrogen peroxide (H_2O_2), are natural byproducts of cellular oxidative metabolism. In addition to endogenous generation within cells, ROS are also produced in response to external stimuli, such as xenobiotics, cytokines, and microbial invasion (17, 18). Intracellular, ROS are primarily produced in mitochondria as a result of the partial reduction of molecular oxygen (O_2) to H_20 during oxidative phosphorylation, a process that generates energy in the form of adenosine triphosphate (ATP). During this process of energy production, electrons leak from the mitochondrial electron transport chain (ETC) and interact with O_2, leading to the formation of $O_2^{\bullet-}$ at complex I and III of the ETC. Besides $O_2^{\bullet-}$, these complexes are also the primary source of H_2O_2 (17, 19). ROS are highly reactive and have a dual role, influencing pathological processes, such as neurodegeneration, cardiovascular malfunctioning, and cancer, or physiological processes, such as immunology, development, neurological functioning, wound healing, and angiogenesis (1). At the physiological level, ROS can act as second messengers, participating in important molecular functions and signal transduction pathways, facilitating the effects of growth factors, cytokines, and calcium signalling. In fact, it is suggested that the ROS-mediated redox (reduction/oxidation) signalling activity

surpasses the extent of ROS-mediated macromolecular damage (18, 20).

Despite being traditionally considered harmful, multiple studies underscored the importance of ROS as signalling molecules that trigger various processes crucial for tissue regeneration. H_2O_2, for instance, can cross cell membranes via aquaporin channels and gap junctions, enabling it to diffuse freely between cells, thereby indicating a signalling function related to this non-radical with a long half-life (1, 3). Following an injury, there is an observed burst of ROS at the site of injury accompanied by prolonged high ROS levels throughout the regeneration process. This suggests pleiotropic biological effects in wound healing and tissue regeneration, as shown in *Xenopus laevis*, zebrafish, and Hydra (1, 21). Love et al. demonstrated in 2013 that injury-induced ROS production, particularly H_2O_2, serves as an important regulator and potential initiator of *Xenopus* tadpole tail regeneration (21). Similarly, Gauron and colleagues revealed that continuous ROS production is essential for triggering cell proliferation and facilitating fin regeneration in zebrafish (22). Furthermore, in Hydra, injury-induced ROS production, especially H_2O_2, coincides with processes such as cell death (apoptosis), migration of interstitial progenitors to the wound site, and a surge in mitotic activity among interstitial cells (23). Upon injury or amputation, planarians also exhibit a dynamic response characterised by a ROS burst at the site of injury. Recently, Jaenen et al. revealed that these injury-produced ROS, especially H_2O_2, are – possible amongst others – essential upstream activators of the MAPK/ERK pathway and thereby help initiate the process of planarian regeneration (3, 16). Furthermore, altered ROS levels were shown to affect patterning and polarity during planarian regeneration. These are fundamental processes of reestablishing an appropriate arrangement and orientation of the regenerating tissue, referred to as 'guided self-organisation' (1, 24). Lastly, recent studies have discussed the role of redox homeostasis in the regulation of stem cell behaviour. Wang *et al.* revealed that ROS play a critical role in determining stem cell fate, showing that stem cells reside in niches characterised by low ROS levels, which are essential for maintaining their self-renewal capacity and stemness, while higher ROS levels induce stem cell proliferation and differentiation. However, a disturbed redox balance, characterised by excessively high ROS levels, can damage stem cells and negatively affect their regenerative capacity (25). These findings underscore the pivotal role of ROS as important signalling molecules orchestrating various cellular processes during regeneration.

The antioxidant system - As previously described, cellular redox signalling has a modulating effect on physiological processes, such as regeneration. However, a disturbed redox balance, as a consequence of excessive ROS accumulation, can lead to oxidative stress, causing direct or indirect macromolecular damage to lipids, proteins, and nucleic acids (e.g., DNA). This ultimately disrupts cellular function and promotes the onset of diverse pathologies (1, 18, 26). To counteract the harmful effects of ROS, cells are equipped with an antioxidant (AOX) defence system. This consists of various antioxidant enzymes, including superoxide dismutase (SOD), catalase (CAT), and glutathione reductase (GR), aimed at maintaining the delicate redox equilibrium by scavenging or detoxifying ROS (27). SOD exemplifies a critical antioxidant enzyme that plays a pivotal role in controlling ROS damage. Functioning as a first line defence against ROS, SOD catalyses the conversion of $O_2^{\bullet-}$ into less reactive species, specifically O_2 and H_2O_2. The catalase, glutathione peroxidase (GPX), and peroxiredoxin (PRX) then convert H_2O_2 into water (28). In addition to enzymatic antioxidants, the AOX system comprises nonenzymatic antioxidants such as the main cellular redox buffer, glutathione (GSH), as well. The balance between reduced GSH and oxidised glutathione disulfide (GSSG) constitutes a critical aspect of cellular redox homeostasis. The GSH pool is maintained through *de novo* synthesis utilising GSH precursors (glutamate, cysteine, and glycine) or through GSH recycling from its oxidised form by the flavin adenine dinucleotide (FAD)-dependent enzyme, GR (27, 29).

During regeneration in *S. mediterranea*, the study of Bijnens and colleagues showed that GSH levels fluctuate dynamically, playing a crucial role in modulating cellular redox balance and antioxidant defence mechanisms to support tissue repair. More specifically, they showed an increase in GSH content at the very beginning of planarian regeneration, which diminishes over time, suggesting a key role in early regeneration stages (30). Additionally, Rosa and colleagues demonstrated that the antioxidant vitamin C promotes regeneration of the planarian *Girardia*

tigrine (31). Similarly, a study by Tsarkova *et al.* revealed that the antioxidant drug Tameron effectively shields *S. mediterranea* from oxidative stress while enhancing regenerative capacity, achieved by modulating the expression of neoblast marker genes and Nuclear factor erythroid 2-related factor 2 (Nrf2)-regulated oxidative stress response genes (32). These recent studies highlight the importance of antioxidants in supporting regenerative processes.

The redox-sensitive molecule, riboflavin - Apart from endogenously synthesised antioxidants, the body also relies on exogenous sources of other redox-sensitive molecules, such as riboflavin (RF), acquired from natural exposures like UV-light and dietary intake of foods rich in this compound, including milk, organ meats (e.g., veal liver), fish, and eggs. RF, also known as vitamin B_2, is a water-soluble vitamin and an essential nutrient for various cellular processes, including energy metabolism, antioxidant defence, and redox regulation (33, 34). RF actively participates in cellular redox reactions as a pivotal precursor for flavin mononucleotide (FMN) and FAD biosynthesis. Upon cellular uptake via the riboflavin transporter (RFT), RF undergoes phosphorylation to form FMN catalysed by riboflavin kinase (RFK), subsequently metabolising into FAD by FMN adenylyltransferase (FMNAT) or FAD synthase (Figure 1). These derivatives, primarily localised in the mitochondria of cells, function as essential cofactors in energy metabolism and serve as coenzymes in aerobic life's redox processes. Specifically, FMN and FAD occupy key positions as important cofactors in the ETC, which influences the amount of generated ROS (33, 35). Furthermore, RF extends beyond its conventional function as a cofactor for flavoproteins in oxidative phosphorylation and ETC reactions, emerging as a redox-sensitive molecule with significant antioxidant properties. For example, it has the ability to scavenge ROS directly through the conversion of its reduced form to its oxidised form (36). Additionally, RF contributes to GSH production through its derivative FAD, which serves as a crucial cofactor in the enzymatic reactions catalysed by GR, facilitating the regeneration of active GSH from its oxidised form, GSSG. By promoting GSH synthesis, RF indirectly enhances cellular antioxidant capacity (33).

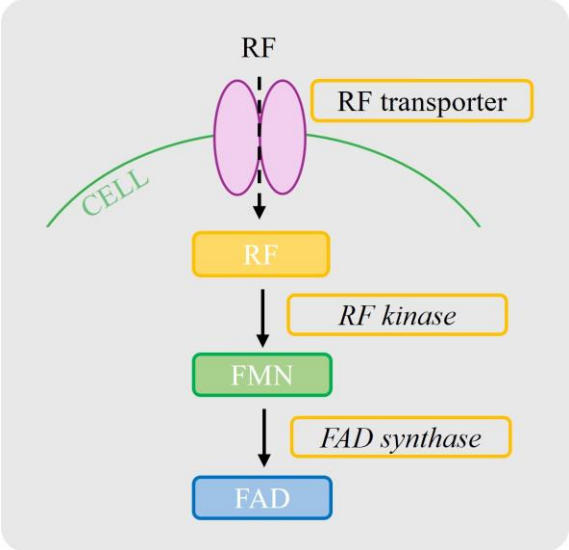

Figure 1: RF transport and metabolism. RF is taken up from the extracellular environment into cells via the RF transporter. Inside the cell, RF is phosphorylated by RF kinase to form FMN, followed by its metabolization into FAD by FAD synthase. *RF, riboflavin; FMN, flavin mononucleotide; FAD, flavin adenine dinucleotide*

Recent undisclosed observations by the BiTElab research group have revealed that the green autofluorescent (AF) signal exhibited by planarians, when excited by blue light, correlates with the AF characteristics inherent to flavins, including RF (Figure 2). Specifically, spectral analysis at 488nm excitation demonstrated that the emission spectrum of the AF signal derived from synthetic flavins is identical to the AF signal exhibited by the planarian. This finding indicates the presence of RF and its derivatives within various tissues and structures of the flatworm. Consequently, the substantial abundance of this redox-sensitive molecule within planarian tissues raises questions into its role in regeneration. However, the functional role of RF in redox-mediated planarian regeneration remains elusive as well as its potential to mediate the AOX response.

The redox-regulating Keap1/Nrf2 pathway - In addition to other conserved mechanisms of maintaining the redox balance, one key regulator of cellular AOX defence, is the redox-regulating Kelch-like ECH-associated protein 1 (Keap1)-Nrf2 pathway in mammals.

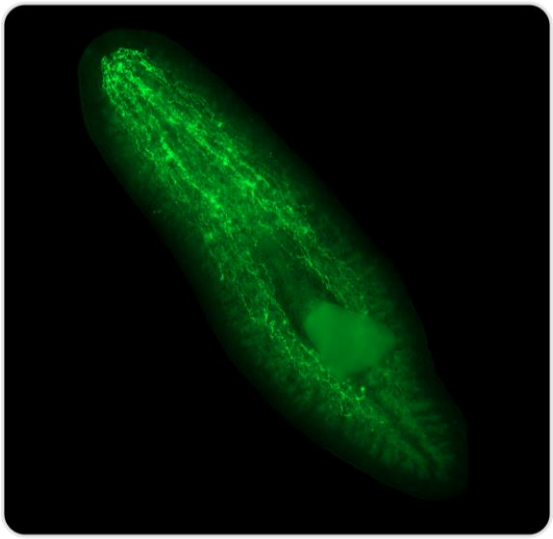

Figure 2: The AF system within the planarian body. Widefield tilescan of the autofluorescence in planarians, visible at 488nm excitation, due to the AF properties of flavins, including RF. This flavin-mediated autofluorescence is primarily observed in the digestive system (gut), together with an interconnected structure, bundled in the head area with lateral branches projecting towards the periphery of the tail. *RF, riboflavin; nm, nanometer*

Under basal conditions, Nrf2 is sequestered in the cytoplasm by the protein sensor, Keap1, which forms part of an E3 ubiquitin ligase and targets Nrf2 for ubiquitination and subsequent proteasomal degradation. However, in response to oxidative or electrophilic stresses, Keap1 undergoes conformational changes, leading to the stabilisation, cellular accumulation, and nuclear translocation of Nrf2 (37, 38). Once in the nucleus, Nrf2 binds to AOX response elements (AREs) in the promoter regions of target genes, thereby inducing the transcription of various antioxidant and cytoprotective enzymes. These include GPX, glutathione S-transferases (GSTs), heme oxygenase 1 (HO-1), NAD(P)H:quinone oxidoreductase 1 (NQO1), SOD, etc.. This orchestrated response enhances cellular AOX capacity, detoxification processes, and maintenance of redox homeostasis (37, 39). Notably, some invertebrates lack the Nrf2 transcription factor, but instead, harbour homologues genes such as Skinhead-1 (SKN-1) in *Caenorhabditis elegans* (*C. elegans*) and Cap "n" collar isoform C (CncC) in *Drosophila melanogaster*. Although SKN-1 regulation is not completely understood, it was shown that SKN-1 shares the role of regulating oxidative stress responses and detoxification pathways with Nrf2, thereby highlighting evolutionary conservation of redox signalling mechanisms across diverse organisms (40, 41).

Purpose - This study aims to gain a deeper understanding of redox-mediated (planarian) regeneration, focusing on the identification, characterization, and functional assessment of alternative redox-sensitive compounds, such as RF and RF-related targets, as well as redox-regulating compounds, such as Keap1 and SKN-1. Our focus will be directed towards investigating the spatio(temporal) dynamics of these molecules in different physiological states in addition to their functional roles during the process of regeneration. We hypothesise that riboflavin is important for the process of regeneration by influencing stem cell dynamics and neuronal development in *S. mediterranea*. In addition, we hypothesize that SKN-1 functions as an Nrf2 homolog in *S. mediterranea*, playing a similar role in the regulation of AOX response mechanisms, and that Keap1 also has a crucial redox-regulating role during planarian regeneration. By gaining deeper insights into redox-mediated planarian regeneration, this study aims to address research gaps in the current understanding of tissue repair, thereby potentially offering foundational insights into biological processes relevant to the advancement of regenerative medicine.

EXPERIMENTAL PROCEDURES

Planarian Cultivation and Amputation - The asexual strain of the planarian *S. mediterranea* was cultivated in a freshwater medium consisting of 1.6 mM NaCl, 1 mM $CaCl_2$, 1 mM $MgSO_4$, 0.1 mM $MgCl_2$, 0.1 mM KCl and 1.2 mM $NaHCO_3$ in milliQ (MQ) water. The planarians were continuously kept in the dark at a constant temperature of 20°C and fed once a week with veal liver for approximately 3-4 hours. Prior to experimental procedures, planarians of similar sizes were selected and starved for at least seven days to avoid food-related effects. Starved planarians are maintained in the laboratory as a continuous resource, obviating the necessity for pre-experimental fasting protocols. To artificially induce planarian regeneration, the planarians were transversely cut between the photoreceptors (eyes) and pharynx, creating regenerating head

and tail segments. To create regenerating trunks, planarians were transversely cut anterior and posterior to the pharynx. This process is called planarian amputation and regenerative stadia are indicated by days post amputation (dpa).

Gene Knockdown via RNA Interference (RNAi) - RNAi is a technique utilised to selectively silence or reduce the expression of specific target genes by neutralising target mRNA, thereby creating genetic knockdowns. In this study, RNAi was performed on planarians to examine the function of certain genes by observing the phenotypic effects on regeneration that result from their knockdown. These genes include *Smed-RFK*, *Smed-RFT*, *Smed-Keap1*, and *Smed-SKN-1*. The GOI sequence of the selected genes was consulted on two databases, NCBI and PlanMine (v3.0), and Primer3 (v4.1.0) was used for RNAi primer design. The primer sequences are summarised in Supplemental Table 1. Primary PCR was then performed followed by gel electrophoresis. The PCR product was cut out of the gel and purified (GeneJET Gel Extraction Kit, Thermo Scientific). Double-stranded RNA (dsRNA) probes were generated by an in vitro transcription system (T7 Ribomax™ Express RNAi System, Promega, Madison, WI, USA) according to the manufacturer's instructions. Finally, purified RNAi probes were diluted to 1500ng/µl and stored at -20°C. Starved, intact animals underwent two cycles of three consecutive micro-injection days over the span of two weeks with three injections per day, each consisting of 32.2nL dsRNA, administered using the Nanoject II (Drummond Scientific, Broomall, PA, USA). Therefore, the planarians were positioned dorsally and injected between the eyes and the pharynx. A corresponding control group received injections of either MQ water or cultivation medium. Subsequently, animals were transversely cut in head and tail (and trunk) segments the day after the final injection to induce regeneration. To study the AF phenotype of planarians following knockdown of *smed-RFK* and *smed-RFT*, live imaging was conducted at 7 dpa and 14 dpa. For this purpose, non-amputated living planarians were immobilised in 2.16 mM linalool in cultivation medium, and images were captured using a Zeiss LSM900 confocal microscope.

Phenotypic Screening and Blastema Size Determination - After planarian amputation, the process of regeneration was followed up to study the effects of gene silencing (RNAi) in comparison to control samples. At 3 dpa, regenerating animals were observed for physical characteristics, focusing on regenerative success, blastema formation and development of the photoreceptors. At 7 dpa and/or 12 dpa, a more thorough phenotypic screening was conducted, involving a behavioural analysis using two cognitive tests (light avoidance test and motility test) in addition to the systematic observation and analysis of physical characteristics including blastema formation and eye development. Eye development was scored as normal, faint or absent. Pictures were taken with a Nikon DS-Ri2 digital camera mounted on a Nikon SMZ800 stereomicroscope. Blastema sizes were determined using Fiji/ImageJ (v2.3.1) and normalised against the total body area of the planarian (μm^2) (Supplemental figure S1).

Behavioural tests - To assess the planarians' cognitive function after gene silencing (RNAi), a motility and light avoidance (LA) test were conducted and the results were compared to those of the control group. The LA test involved placing planarians individually in a cultivation medium-filled dish (60x30 mm) divided in four quadrants (Q0-3) and exposing them to a bright light source. After an acclimatisation period of twenty seconds in the brightest quadrant (Q0), their movement away from the light was monitored for a duration of ninety seconds. This test assessed the planarian's photophobic behaviour by measuring the percentage of time spent in the darkest quadrant (Q3). Conversely, the motility or planarian locomotive velocity (pLMV) assay measured the spontaneous locomotor activity of planarians by tracking their movements in a cultivation medium-filled petri dish placed upon 0.5 cm grid paper for ninety seconds, again after an acclimatisation period of twenty seconds. The number of lines crossed or recrossed was then multiplied by a factor of 3.33, thereby estimating the number of lines crossed in five minutes.

DETC exposure - To investigate the functional impact of *Smed-Keap1* and *Smed-SKN-1* knockdown on planarian regeneration in context of oxidative stress, we employed RNAi followed by exposure to diethylthiocarbamate (DETC, Sigma-Aldrich, Cat. No. 228680), a known inhibitor of SOD. Planarians were subjected to RNAi treatment targeting *Smed-Keap1* and *Smed-SKN-1*. Following the third and

final injection, planarians were transversely cut between the eyes and pharynx to induce regeneration. Post-amputation, half of the RNAi-treated planarians were allowed to regenerate in normal cultivation medium, while the other half were exposed to 0.3µM DETC-containing medium to induce oxidative stress. At 3 dpa and 7 dpa, regenerating animals were observed for physical characteristics, focusing on regenerative success, blastema formation and development of the photoreceptors.

Whole-Mount Fluorescent In Situ Hybridisation (FISH) – Whole-mount FISH was used to study the spatial expression patterns of selected genes in the planarian body, during regeneration, and in response to gene silencing. The gene of interest is *smed-RFT*. The GOI sequence of this selected gene was consulted on two databases, NCBI and PlanMine (v3.0), and Primer3 (v4.1.0) was used for primer design. The primer sequences are summarised in Supplemental Table 1. Primary PCR was then performed followed by gel electrophoresis. The PCR product was cut out of the gel and purified (GeneJET Gel Extraction Kit, Thermo Scientific). Probes were synthesised using the DIG RNA (SP6/T7) Labelling Kit from Roche, according to the manufacturer's instructions, starting from a purified PCR product of the gene of interest. The expression patterns of *Smed-RFT*, tyrosine hydroxylase (TH), and prohormone convertase 2 (PC2) were assessed following the protocol outlined by King and Newmark in 2013, which is briefly explained in the Supplemental experimental procedures (42). Images were captured using a Zeiss LSM900 confocal microscope.

Whole-Mount Immunohistochemistry (IHC) - We used whole-mount IHC as a staining technique to detect and visualize specific antigens (proteins) of interest within planarian tissues. After RNAi treatment, mitotically active stem cells were stained as described by Plusquin *et al.*, 2012 (43). Therefore, the primary antibody against phosphorylated Histone-H3 at serine 10 (D2C8, rabbit mAb, Cell-Signalling, Danvers, MA, USA, Cat. No. 3377S, diluted 1:1000) was used, together with the secondary goat anti-rabbit-IgG Alexa Fluor 568-conjugated antibody (Thermo Fisher Scientific, Cat. No. A-11036, diluted 1:500). Following mounting in ImmuMount (Thermo Fisher Scientific), pictures were taken using a Zeiss LSM900 confocal microscope. The total number of mitotic stem cells was counted using Fiji/ImageJ (v2.3.1) and normalised against the total body size of the worm (μm^2).

For the co-localization with stem cells, we employed a combined FISH and immunostaining protocol for the general stem cell marker, *Smedwi*-1 (Supplemental experimental procedures). Differences in regeneration of the CNS were assessed by performing an immunostaining using anti-SYNORF-1 (Supplemental experimental procedures).

Expression analyses from Publicly Available Data - Using the PlanMine (v3.0, MPI-CBG, Dresden, Germany) database (44), publicly available information regarding the spatial, cell-type specific and temporal gene expression patterns of several genes was consulted. For each transcript, the search was restricted to the organism *S. mediterranea* and the dataset dd_smed_v6.

Statistical Analysis - Blastema sizes, stem cell counts, photoreceptor and cognitive data, ganglia and fluorescence intensity measurements were analysed in GraphPad Prism 10.2.3.403. A normal distribution was assessed using the Shapiro-Wilk test ($p < 0.05$). Significant differences between the test condition and control group as well as between test conditions were assessed using an unpaired t-test ($p < 0.05$). When assumptions of normality were not met, a Mann-Whitney test ($p < 0.05$) was performed.

RESULTS

Knockdown of the RF kinase gene reduces the size of newly formed tissue and impairs photoreceptor development in RNAi-treated tails. To get a first indication into the potential role of RF, members related to its metabolism and transport were selected and their expression profiles, obtained from PlanMine (v3.0), were examined. The lineage trees associated with our genes of interest display the specific cell types expressing *Smed-RFK* and *Smed-RFT* (Figure 3d). These indicate that *Smed-RFK* is expressed in, among others, neuronal cell types and glial cells, suggesting a potential role in the development of the planarian's nervous system. On the other hand, *Smed-RFT* is primarily expressed in glial cells. Next, RNAi was employed for the targeted silencing of *Smed-RFK* and *Smed-RFT* to gain a better understanding of the functional role of RF during regeneration. Our

results show that silencing of the *Smed-RFK* gene significantly reduces blastema size in RNAi-treated tails at 7 dpa compared to the controls ($p < 0.01$). However, no significant reduction in blastema size was observable in *Smed-RFK*-RNAi treated heads nor in *Smed-RFT*-RNAi treated heads or tails, compared to the control group (Figure 3c). Furthermore, eye development was examined and scored at 7 dpa. In the control group, 66.67% of planarians developed normal eyes, 25% had faint eyes, and 8.33% had no eyes. In the *Smed-RFK*-RNAi group, only 18.18% of planarians developed normal eyes, 45.45% had faint eyes, and 36.36% had no eyes. Conversely, in the *Smed-RFT*-RNAi group, 75% of planarians developed normal eyes, and 25% had faint eyes, with no instances of absent eyes observed. This indicates that while *Smed-RFT* knockdown does not significantly impair eye development in comparison with the control group, *Smed-RFK* knockdown does (Figure 3b).

Silencing of RF kinase and the RF transporter affects RF distribution within the planarian body. In *S. mediterranea*, flavin-mediated autofluorescence is primarily observed in the gut, and within an interconnected neuronal-like structure that is bundled in the head area and extends toward the tail. In addition to observing an AF signal in the gut and neuronal-like structure, a general green background is present both dorsally and ventrally across all tissue layers (Figure 2). To gain a better understanding of RF availability within the planarian body following silencing of RF-related targets, the AF system exhibited by planarians was examined. Compared to the AF system illustrated in Figure 2, all RNAi-treated planarians exhibit a less prominent and intense AF signal, likely due to the starvation period preceding the experimental procedures (Figure 3c). Furthermore, our findings revealed distinct alterations in the distribution of RF, and its availability, following knockdown of the *Smed-RFK* and *Smed-RFT* genes. Specifically, at 14 dpa, we observed little to no AF signal in the blastema of *Smed-RFK*-RNAi treated tails, both ventrally and dorsally, compared to the controls (Figure 3c). Furthermore, at 7 dpa, inhibition of *Smed-RFT* led to a disruption in RF distribution throughout the planarian body in comparison with the control group, with a notable reduction in RF content within the neuronal-like structure (ventral) and an accumulation of RF in the epidermis (dorsal) (Figure 3c).

Knockdown of the RF transporter gene reduces the number of mitotically active stem cells in RNAi-treated heads. To investigate the potential importance of RF for stem cell proliferation, we employed RNAi to silence the *Smed-RFK* and *Smed-RFT*. At 3 dpa, an immunolabelling for H3P was conducted to evaluate the impact of gene inhibition on the number of mitotically active stem cells. Compared to the controls, our observations revealed that inhibition of *Smed-RFK* did not yield a significant effect on this number of mitotic stem cells in both regenerating heads and tails (Figure 4). Meanwhile, inhibition of *Smed-RFT* resulted in a significant reduction of $H3P^+$ cells in treated heads ($p < 0.0001$) in comparison with the number of $H3P^+$ cells observed in control heads. Lastly, no significant reduction or increase was observed in the amount of mitotically active stem cells in *Smed-RFT*-RNAi treated tails (Figure 4).

Inhibition of RF kinase affects the development of dopaminergic neurons. The impairment of eye formation observed following *Smed-RFK*-RNAi at 7 dpa suggests a disruption in neural development pathways (Figure 3b). To investigate this further, a FISH was conducted targeting SERT, a marker for serotonergic neurons and TH, a marker for dopaminergic neurons, after *Smed-RFK*-RNAi at 12 dpa. Regrettably, the SERT staining was unsuccessful, precluding any observations regarding the impact of *Smed-RFK* knockdown on the development of serotonergic neurons. Fortunately, the TH staining was successful, allowing us to study the expression pattern of this neuronal marker following *Smed-RFK* knockdown. In the control heads, ventral TH expression was observed within the cephalic ganglia (brain), whereas dorsally, TH expression was confined to the peripheral epidermal layer of the head, corresponding with the subepidermal nerve plexus (Figure 5b). Following *Smed-RFK* knockdown, our findings revealed notable alterations in TH expression patterns compared to controls. Ventral TH expression within the cephalic ganglia shifted peripherally in comparison with the control. Additionally, dorsal TH expression appeared to be dispersed within the epidermal layer of the newly formed tissue, in contrast to the control where such expression is not observed (Figure 5b). Moreover, a motility and light avoidance test

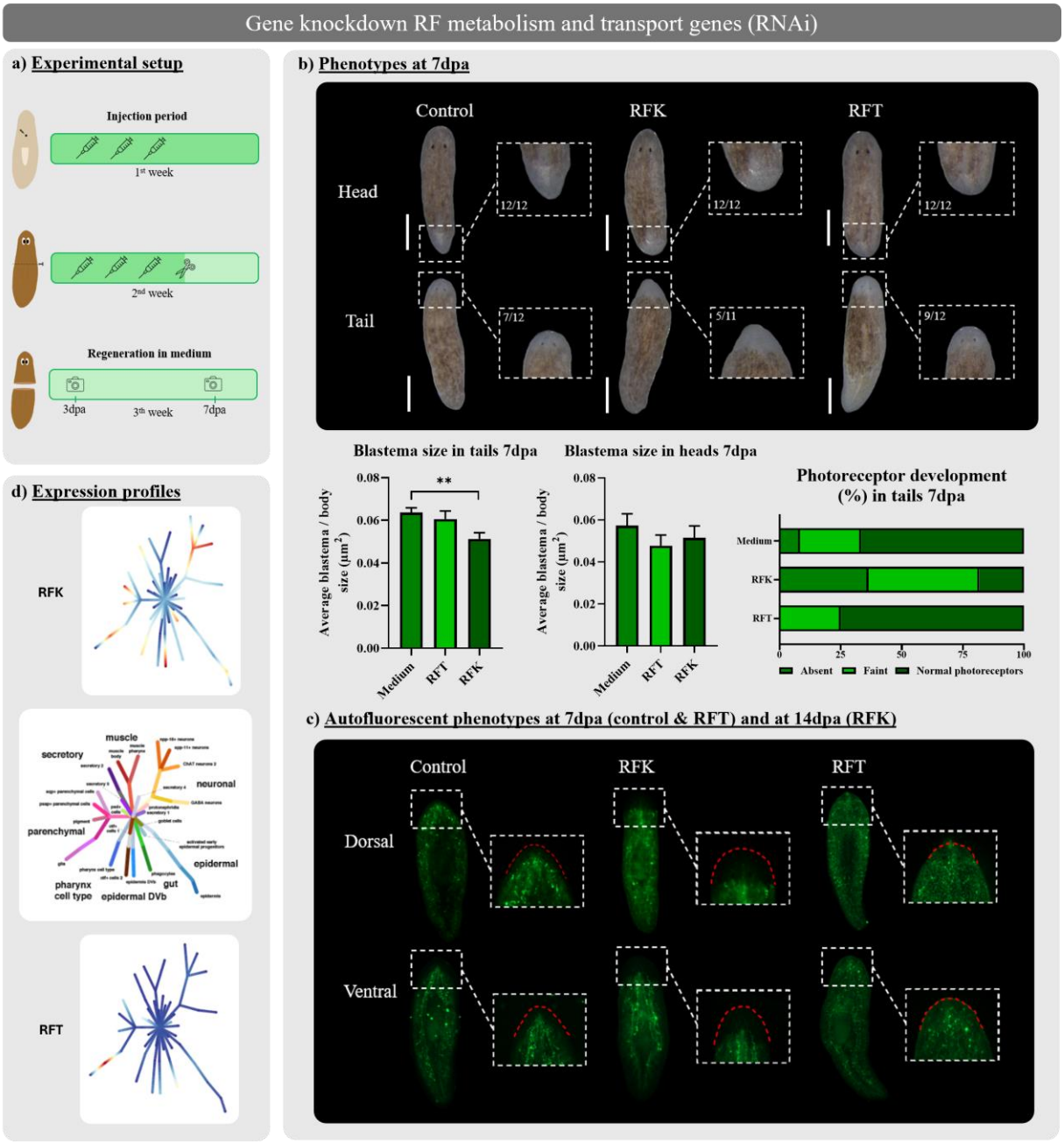

Figure 3: Effects of RF kinase and RF transporter knockdown on planarian regeneration. a) Overview of the experimental setup: planarians were transversely cut between the eyes and pharynx the day after the final injection to induce regeneration. Pictures were taken at 3 dpa and 7 dpa for blastema measurements and morphological analysis of the photoreceptors. **b)** Phenotypes of regenerating heads and tails at 7 dpa after RNAi treatment targeting *Smed-RFK* and *Smed-RFT*. Scale bars of 1000 µm. The numbers above each worm indicate the frequency of the observed phenotype relative to the total number of observations. Bar graphs below show the average blastema-to-body size ratio of regenerating heads and tails at 7 dpa. Statistical significance is indicated by: **p<0.01. Photoreceptor development in regenerating tails at 7 dpa is shown on the right. **c)** Autofluorescent phenotypes at 7 dpa of controls and after RNAi treatment targeting *Smed-RFT*, and at 14 dpa after RNAi treatment targeting *Smed-RFK*. **d)** Expression profiles of the selected genes, obtained from the PlanMine 3.0 database. Abbreviations: *RF, riboflavin; RNAi, RNA interference; dpa, days post amputation; RFK, riboflavin kinase; RFT, riboflavin transporter; µm, micrometer.*

were conducted to assess cognitive function in planarians following *Smed-RFK*-RNAi at 12 dpa. The results demonstrate that *Smed-RFK* knockdown negatively impacts planarian motility ($p < 0.0001$) and their response to environmental stimuli ($p < 0.01$), here being a light stimulus (Figure 5c).

Furthermore, to investigate the effects of RF knockdown on neurodevelopment we targeted RF by simultaneously inhibiting the expression of the *Smed-RFK* and *Smed-RFT* using RNAi. At 7 dpa, we performed an immunolabeling for the CNS, consisting of a pair of cephalic ganglia and a pair of longitudinal ventral nerve cords (VNCs) running along the animals' length, employing an anti-synapsin antibody. No significant decreasing trend in ganglia regeneration could be observed in regenerating tails compared to controls (Supplemental Figure 2). Additionally, we examined the presence of an anterior commissure between the two cephalic ganglia. All RF-RNAi treated animals displayed the presence of this commissure as well as the animals of the control group (Supplemental Figure 2).

The RF transporter is expressed in stem cells and at the wound site during early regeneration stages. The reduction in the number of mitotic stem cells observed following *Smed-RFT* knockdown suggests the involvement of RF in stem cell dynamics (Figure 4). To elucidate this further, the potential expression of *Smed-RFT* in stem cells was assessed. A co-localization was performed by optimising an existing FISH protocol targeting *Smed-RFT* followed by an immunolabelling for the general stem cell marker *Smedwi-1*. This revealed the expression of *Smed-RFT* in stem cells (Figure 6a). Subsequently, we characterised the spatio-temporal expression pattern of *Smed-RFT* during early regeneration. A FISH conducted at 6 hours post amputation (hpa) and 3 dpa revealed the expression, of *Smed-RFT* near the wound site at 6hpa, suggesting its involvement in early regeneration stages (Figure 6b).

Smed-Keap1 and the Nrf2 functional homolog Smed-SKN-1 are expressed in the planarian genome. An examination of PlanMine (v3.0) data indicated that the transcription factor Nrf2 is not expressed in *S. mediterranea*, whereas *Smed-Keap1* is. However, given the functional homology of SKN-1 to Nrf2 in *C. elegans*, an inquiry arose regarding its expression in planarians. Subsequent analysis confirmed the expression of *Smed-SKN-1* in *S. mediterranea*. Multiple RNAi probes were designed for both *Smed-Keap1* and *Smed-SKN-1* (Supplemental Table 1). The lineage trees associated with our genes of interest display the specific cell types expressing *Smed-Keap1* and *Smed-SKN-1*. *Smed-Keap1* is primarily expressed in neuronal cell types in addition to pharyngeal muscle cells (Figure 7e). The first transcript of *Smed-SKN-1* is predominantly expressed in the epidermis, including the dorsal-ventral boundary (DVb). Finally, while the second *Smed-SKN-1* transcript is expressed in a wide array of cell types, including neuronal, epidermal, and pharyngeal cell types, expression of the third *Smed-SKN-1* transcript is limited to secretory cell types (Figure 7e).

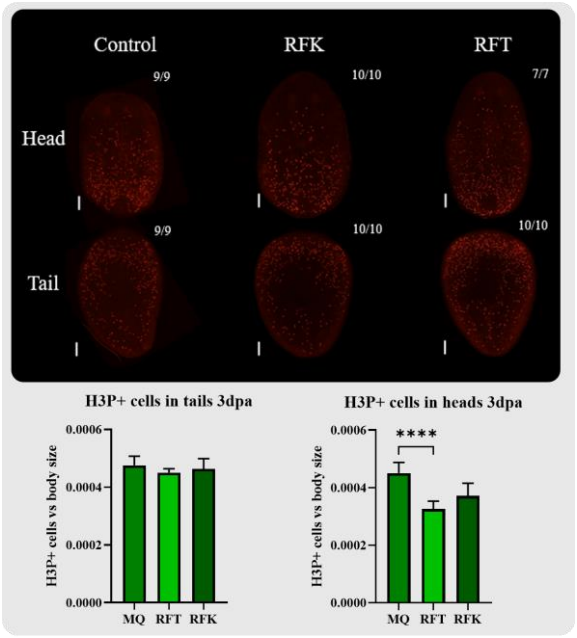

Figure 4: Stem cell proliferation at 3 dpa following knockdown of RF-related targets (RNAi). At 3 dpa, regenerating heads and tails were stained for H3P as a measure of stem cell proliferation. Scale bars of 1000 µm. The numbers above each worm depict the frequency of the observed phenotype relative to the total number of observations. Bar graphs below show the relative number of $H3P^+$ cells normalized to body size in regenerating heads and tails. Statistical significance is indicated by: ****$p<0.0001$. Abbreviations: *dpa, days post amputation; RFK, riboflavin kinase; RFT, riboflavin transporter; H3P, phosphohistone H3; MQ, MilliQ; µm, micrometer.*

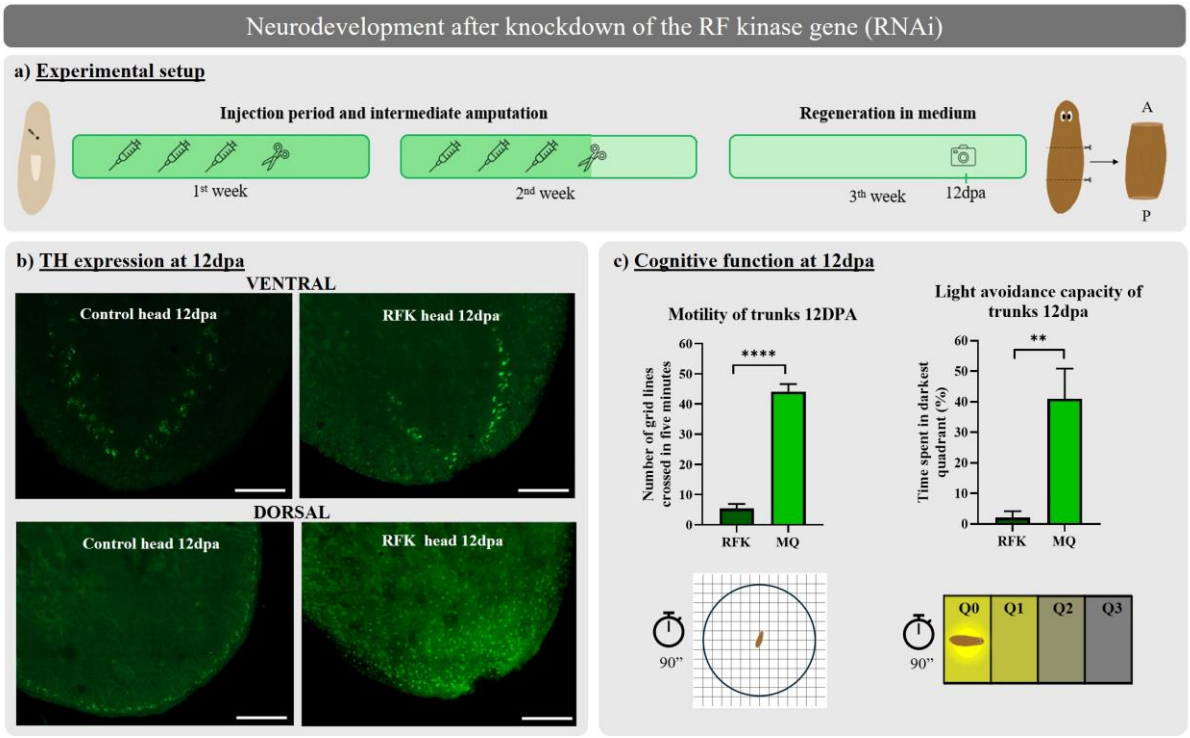

Figure 5: Neuronal development during planarian regeneration following RNAi-mediated knockdown of RF kinase. a) Overview of the experimental setup: planarians were transversely cut posterior and anterior of the pharynx the day after the third and final injection to induce regeneration. At 12 dpa, pictures were taken, and a motility and light avoidance test were conducted. **b)** At 12 dpa, regenerating trunks were fixed and stained for the dopaminergic marker, TH. Confocal images display ventral and dorsal TH expression patterns in the anterior (head) region of regenerating trunks. Scale bars of 100 µm. **c)** Behavioural analysis of regenerating tails at 12 dpa after RNAi treatment targeting *Smed-RFK*. Bar graphs show the planarians' relative performance during the motility and light avoidance test. Experimental setups are illustrated below. Statistical significance is indicated by: **p<0.01, ****p<0.0001. Abbreviations: *RF, riboflavin; RNAi, RNA interference; dpa, days post amputation; RFK, riboflavin kinase; TH, tyrosine hydroxylase; A, anterior; P, posterior; Q, quadrant.*

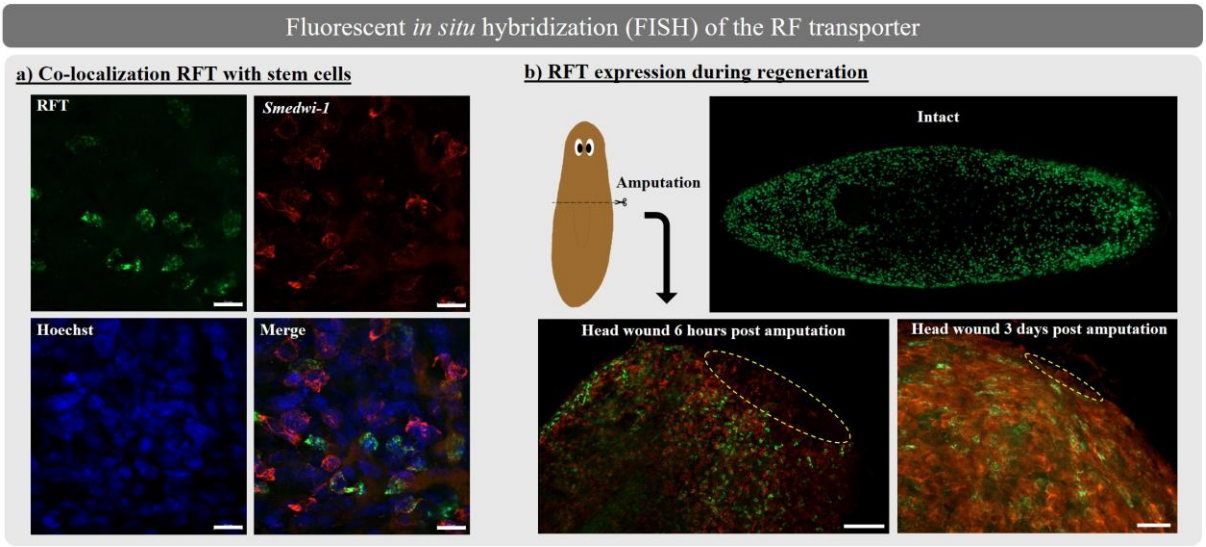

Figure 6: Expression pattern of the RF transporter in stem cells and during planarian regeneration. a) Planarians were fixed and stained for *Smed-RFT* (green, 488nm) using FISH,

combined with immunostaining for the general stem cell marker, *Smedwi-1* (red, 586nm). Nuclei were stained with Hoechst (blue, 508nm). The merged image is shown on the right below. Scale bars of 10 µm. **b)** Following amputation, planarians were fixed and stained for *Smed-RFT* (green) and *Smedwi-1* (red) at six hours and three days after cutting. The circled area (yellow) represents the wound site. Scale bars of 100 µm (left) and 20 µm (right). The top image shows the expression pattern of *Smed-RFT* within the intact planarian body. Abbreviations: *RF, riboflavin; RFT, riboflavin transporter; nm, nanometer; µm, micrometer*.

Knockdown of Smed-Keap1 and Smed-SKN-1 does not significantly affect blastema formation and photoreceptor development. To investigate the functional roles of *Smed-Keap1* and *Smed-SKN-1* in planarian regeneration, we initially conducted a gene knockdown experiment targeting these genes using RNAi. The results show that the silencing of these genes does not significantly affect the formation of new tissue nor the development of photoreceptors (Figure 7b,d). To examine the effects of *Smed-Keap1* and *Smed-SKN-1* knockdown on cognitive function, we conducted a motility and light avoidance test. In comparison to the control group, the motility of regenerating tails exhibited significant differences across all targets groups, except for those subjected to *Smed-Keap1_1* knockdown (Figure 7c). Specifically, planarians treated with Keap1_2 ($p < 0.05$), SKN1_1 ($p < 0.05$), and SKN1_3 ($p < 0.01$) displayed impaired motility relative to controls, whereas those subjected to *Smed-SKN1_1* knockdown demonstrated significantly enhanced motility ($p < 0.0001$). In the light avoidance test, planarians with *Smed-Keap1_2* knockdown exhibited an improved response to intense light ($p < 0.05$), whereas those treated for SKN1_1 showed minimal response to this stimulus ($p < 0.01$) (Figure 7c). Conversely, the performance of other groups did not significantly deviate from that of the control group. These results, somewhat divergent from our initial expectations, warrant further investigation.

Furthermore, to investigate the effects of *Smed-Keap1* and *Smed-SKN-1* knockdown on neurodevelopment we inhibited *Smed-Keap1* by simultaneously injecting the Keap1_1 and Keap1_2 targets, and *Smed-SKN-1* by simultaneously injecting the SKN1_1, SKN1_2, and SKN1_3 targets using RNAi. At 7 dpa, we performed an immunolabeling for the CNS, employing an anti-synapsin antibody. Compared to the control group, no significant difference in ganglia regeneration could be observed in regenerating tails (Supplemental Figure 2). Additionally, we examined the presence of an anterior commissure between the two cephalic ganglia. All RNAi treated animals displayed the presence of this commissure as well as the animals of the control group (Supplemental Figure 2). Lastly, we conducted a FISH for the neuronal markers PC2 and TH following separate knockdowns of the *Smed-Keap1* and *Smed-SKN-1* related targets to further investigate the impact of gene knockdown on neurodevelopment. No images are available for PC2 expression after *Smed-SKN1_3* knockdown and for TH expression in all *Smed-SKN-1*-RNAi treated samples. The control group, analysed by PC2 FISH, displayed the cephalic ganglia. This expression pattern was comparable to that observed after knockdown of *Smed-Keap1_1*, *Smed-SKN1*_1, and *Smed-SKN1_2*, with the exception of the *Smed-Keap1_2*-RNAi treated regenerating tails, which exhibited a smaller brain (Supplemental Figure 2). This discrepancy following *Smed-Keap1_2* knockdown was also evident regarding TH expression, as these regenerating tails showed reduced expression in the cephalic ganglia compared to controls. TH expression following *Smed-Keap1_1* knockdown was similar to that of the control group (Supplemental Figure 2). Furthermore, the total amount of stem cells was visualised employing *Smedwi-1* immunolabelling. No significant differences in *Smedwi-1* expression were observed compared with the controls (Supplemental Figure 2).

DETC-induced oxidative stress causes a stress phenotype in early regeneration stages and is not compensated following knockdown of Smed-Keap1 and Smed-SKN-1 related targets. To study the functional role of *Smed-Keap1* and *Smed-SKN-1* during regeneration in function of their redox-regulating capacity, we designed and performed a functional experiment where we induced oxidative stress by exposing planarians to DETC, an inhibitor of the SOD enzyme. By inhibiting SOD, we aimed to reduce the AOX response, thereby amplifying oxidative stress, allowing us to evaluate its impact on blastema formation and photoreceptor development during regeneration after silencing *Smed-Keap1* and *Smed-SKN-1*.

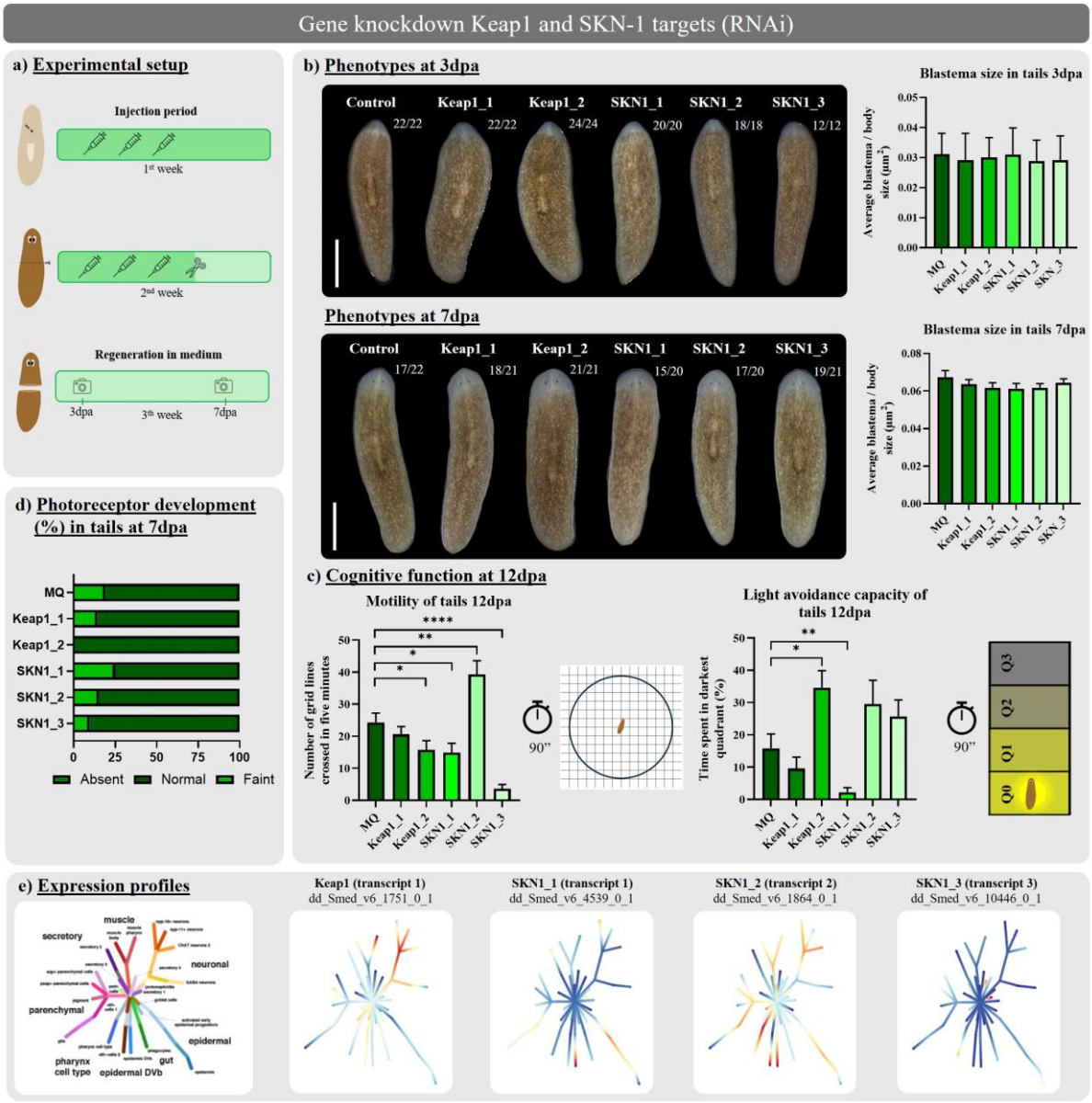

Figure 7: Effects of *Smed-Keap1* and *Smed-SKN-1* knockdown on planarian regeneration. a) Overview of the experimental setup: planarians were transversely cut between the photoreceptors (eyes) and pharynx the day after the final injection to induce regeneration. Pictures were taken at 3 dpa and 7 dpa for blastema measurements and morphological analysis of the photoreceptors. **b)** Phenotypes of regenerating tails at 3 dpa and 7 dpa after RNAi treatment targeting *Smed-Keap1* and *Smed-SKN-1*. Scale bars of 1000µm. The numbers above each worm indicate the frequency of the observed phenotype relative to the total number of observations. Bar graphs display the average blastema-to-body size ratio of regenerating tails. **c)** Photoreceptor development in regenerating tails at 7 dpa. **d)** Behavioural analysis of regenerating tails at 12 dpa after RNAi treatment targeting *Smed-Keap1* and *Smed-SKN-1*. Bar graphs depict the planarians' relative performance during the motility and light avoidance tests. Experimental setups are illustrated on the right. Statistical significance is indicated by: *p<0.05, **p<0.01, ****p<0.0001. **e)** Expression profiles of the selected genes, obtained from the PlanMine 3.0 database. Abbreviations: *RNAi, RNA interference; Keap1, Kelch-like ECH-associated protein 1; SKN-1, Skinhead-1; Q, quadrant; dpa, days post amputation; µm, micrometer.*

The phenotypes at 3 dpa indicate the presence of some sort of stress phenotype as a result of DETC exposure (Figure 8b). DETC-exposed planarians exhibit a shrunken phenotype,

whereas the non-exposed planarians, which are kept in cultivation medium, do adopt an elongated shape (Figure 8b). In the control heads, at 3 dpa, DETC exposure did not significantly affect blastema size, whereas in heads treated with *Smed-Keap1*-RNAi and *Smed-SKN*1-RNAi it significantly reduced blastema size compared to non-exposed planarians ($p < 0.01$). No significant effects on blastema size were found in regenerating tails at 3 dpa (Figure 8b). Regarding an additional comparison between the three RNAi treatment groups, no significant difference could be observed when comparing the control group with the *Smed-Keap1*-RNAi treated group nor with the *Smed-SKN-1*-RNAi treated group in both regenerating heads and tails at 3 dpa (Figure 8b).

At 7 dpa, in the control and *Smed-SKN-1*-RNAi treated regenerating heads and tails, DETC exposure did not significantly affect blastema size, whereas a significant reduction in blastema size was found in DETC-exposed *Smed-Keap1*-RNAi treated heads ($p < 0.05$),

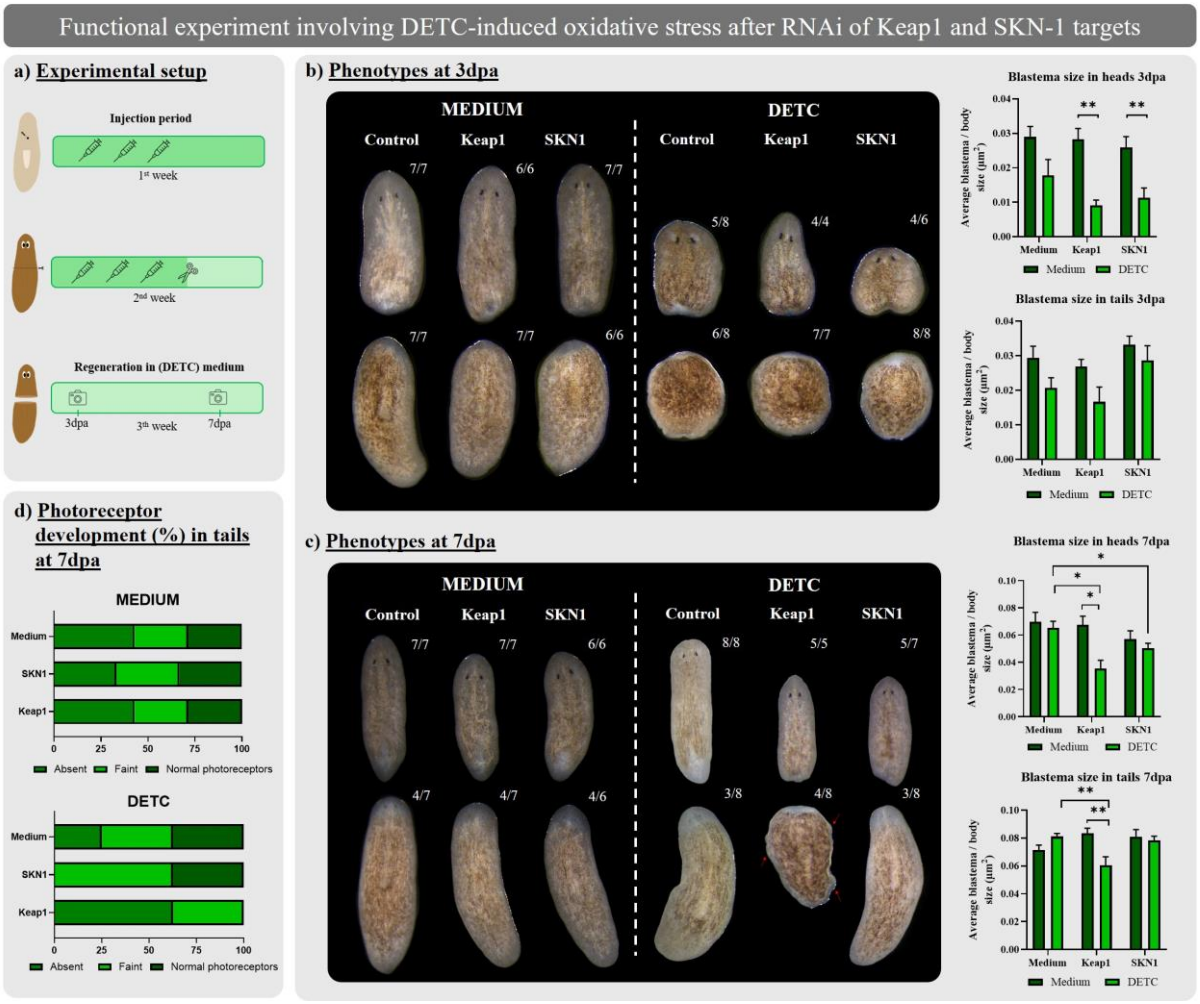

Figure 8: Effects of *Smed-Keap1* and *Smed-SKN-1* knockdown on planarian regeneration under oxidative stress conditions induced by DETC. a) Overview of the experimental setup: planarians were transversely cut between the photoreceptors (eyes) and pharynx the day after the final injection to induce regeneration. Half of the planarians were allowed to regenerate in cultivation medium, while the other half were exposed to DETC. Pictures were taken at 3 dpa and 7 dpa for blastema measurements and morphological analysis of the photoreceptors. **b-c)** Phenotypes of regenerating heads and tails at 3 dpa and 7 dpa. The numbers above each worm indicate the frequency of the observed phenotype relative to the total number of observations. Bar graphs display the average blastema-to-body size ratio of regenerating tails. Statistical significance is indicated by: *p<0.05, **p<0.01. **d)** Photoreceptor development in regenerating tails at 7 dpa. Abbreviations: *DETC, Diethyldithiocarbamate; RNAi, RNA interference; Keap1, Kelch-like ECH-associated protein 1; SKN-1, Skinhead-1; dpa, days post amputation; µm, micrometer.*

as well as in DETC-exposed *Smed-Keap1*-RNAi treated tails ($p < 0.01$) (Figure 8c). The presence of a stress phenotype, accompanied with blister formation, was solely observable for the *Smed-Keap1*-RNAi treated tails (Figure 8c). Furthermore, at 7 dpa, we observed a significant difference between the control group and the *Smed-Keap1*-RNAi treated group ($p < 0.05$), as well as between the control group and the *Smed-SKN-1*-RNAi treated group ($p < 0.05$) in regenerating heads. This significant difference was also observable in regenerating tails when comparing the control group and *Smed-Keap1*-RNAi treated group ($p < 0.01$) (Figure 8c). Moreover, differences in photoreceptor development at 7 dpa between the DETC-exposed and non-exposed (medium) groups were observable (Figure 8d). For the non-exposed planarians, results between RNAi treatment groups were similar as one-third developed no eyes, one-third faint eyes, and one-third normal eyes. These results were comparable to the results of the exposed control group, while the majority of exposed *Smed-SKN-1*-RNAi treated tails developed faint eyes. Non of the exposed *Smed-Keap1*-RNAi treated tails developed normal eyes with the majority not developing eyes at all (Figure 8d).

DISCUSSION

The intricate process of animal regeneration, governed by a tightly regulated network of signalling pathways, remains a captivating yet incompletely understood phenomenon. Planarians, particularly *S. mediterranea*, have emerged as ideal models to study regeneration and were also used in this study as an entry point to investigate redox-mediated regeneration (3). While regeneration research often focuses on unravelling the roles of reactive oxygen species (ROS) or antioxidants (AOXs) in regeneration, the involvement of other redox-sensitive or redox-regulating compounds has been inadequately studied. This exploratory study aims to elucidate the functional role of riboflavin (RF) in planarian regeneration and, to our knowledge, is the first to investigate the involvement of the redox-regulating proteins Keap1 and SKN-1.

The forgotten redox-sensitive vitamin RF, that has a crucial role in cellular metabolism and mainly serves as a coenzyme for a variety of flavoprotein enzymes in the form of its derivatives FMN and FAD, was shown to have significant antioxidative properties in addition to anti-inflammatory, anti-aging, and anti-cancer properties (33, 36). However, within the context of planarian regeneration, the functional role of RF is unknown. The experimental manipulation of the genes encoding for RFK and RFT, responsible for the metabolism and transport of this vitamin, via RNAi sheds light on their functional significance during planarian regeneration. Our results demonstrate that knockdown of *Smed-RFK* significantly reduces blastema size and photoreceptor development in regenerating tails, whereas knockdown of *Smed-RFT* does not yield such effects (Figure 3b). This indicates that RF metabolization into its derivatives via RFK is essential for successful regeneration. The importance of RF metabolism in tissue regeneration is probably due to RF's antioxidative properties. RF is able to influence the levels of important antioxidant enzymes, including SOD, CAT and GPX, as well as acting as an antioxidant itself, capable of directly scavenging ROS. Additionally, its derivative FAD is crucial for the GR system, supporting the importance of RF metabolism for the AOX response necessary for effective tissue regeneration (33). Furthermore, RF's derivatives, FMN and FAD, are primarily located in mitochondria, where they play crucial roles in energy metabolism (35). Adenosine triphosphate (ATP) serves as the primary source of cellular energy, and it has been suggested that the modulation of oxidative metabolism to elevate ATP levels could help address the high energetic requirements associated with enhanced anabolic biosynthesis, mitosis, and migration during tissue regeneration (45). Wang *et al.* demonstrated that RF supplementation in hypoxic mice improved energy metabolism (46). The different observations in photoreceptor development suggest that this process might be more dependent on RF metabolism via RFK than on RF transport via RFT (Figure 3b). This impaired photoreceptor development following depletion of RF levels aligns with other research findings that reveal the causal effects of RF deficiency for various ocular pathologies (47, 48).

The flavin-mediated AF signal allowed us to study RF distribution within the planarian body following knockdown of *Smed-RFK* and *Smed-RFT*. Compared to the planarian's autofluorescence illustrated in Figure 2, the RNAi-treated controls exhibit a less prominent and intense AF signal (Figure 3c). This can be

attributed to the seven-day starvation period preceding experimental procedures, given that planarians obtain RF exclusively from dietary sources (e.g., veal liver) (33, 34). Following *Smed-RFK* knockdown, which impairs the metabolization of RF into its derivatives FMN and FAD, little to no AF signal could be observed in the newly formed tissue (Figure 3c). While this might indicate that the AF signal of the blastema is rather flavin-mediated than RF-mediated, this conclusion cannot be made for the old tissue, as we cannot exclude the presence of RF, FMN, and FAD in this tissue. The possibility of autofluorescence being rather flavin-mediated was supported by a study investigating the molecular origin of the autofluorescence exhibited by *Eisenia fetida* and concluded that either RF or FMN is the molecular source of this AF signal (49). The expression profile of *Smed-RFK*, showing that this gene is expressed in glial cells and neuronal cell types, indicates that RF metabolism is potentially important for neuronal regeneration (Figure 3d). To further investigate this hypothesis, we studied the effects of *Smed-RFK* knockdown on dopaminergic neuronal expression and cognitive function. The results indicate that *Smed-RFK* is indeed essential for successful neuronal development (Figure 5). Given that FAD levels depend on the activity of RFK and FAD functions as a vital co-enzyme for monoamine oxidase (MAO), which is a metabolising flavoenzyme responsible for the oxidative deamination of free (mono)amines (serotonin, dopamine, octopamine) located at the nerve terminal of (mono)aminergic neurons, this impaired neurodevelopment can potentially be attributed to insufficient neuronal functionality as a result of FAD-depletion (50, 51). The observation of impaired eye development after *Smed-RFK* knockdown further enhances this hypothesis since the monoamine, serotonin, was found to be essential for eye regeneration in *S. mediterranea* (Figure 3b) (52). It would be interesting to conduct a staining for the serotonergic marker, SERT, after *Smed-RFK*-RNAi to study the development of these neurons.

Following *Smed-RFT* knockdown, we observed an accumulation of RF in the epidermis where such expression is normally not observed as supported by the expression profile of *Smed-RFT* (Figure 3c,d). Knockdown of *Smed-RFT* would hinder cellular uptake of RF from phagocytes of the gut into target tissues, such as glial cells, which might lead to an increased concentration of RF remaining in peripheral tissues. Additionally, the neuronal-like structure was less developed following *Smed-RFT* knockdown, possibly due to the unavailability of RF in glial cells, suggesting a potential role in neurodevelopment. This is further supported by the fact that RFT deficiency in humans, caused by a loss-of-function mutation in the genes encoding for riboflavin transporters 2 and 3, leads to a progressive neurodegenerative disease (53). To study whether stem cell proliferation during planarian regeneration is affected by knockdown of RF-related targets, an H3P immunostaining was performed to visualize mitotically active stem cells. Our data shows that the number of proliferating cells was significantly lower in regenerating heads after *Smed-RFT* silencing (Figure 4). In *Drosophila*, glial cells regulate neuroblast proliferation in response to systemic nutritional cues, suggesting that *Smed-RFT* is potentially important for stem cell proliferation by ensuring the availability of RF in glial cells (54). To further investigate this finding, we conducted a co-localization of *Smed-RFT* and the general stem cell marker, *Smedwi-1*, revealing the expression of *Smed-RFT* in stem cells. Additionally, the expression pattern of *Smed-RFT* during regeneration reveals *Smed-RFT* expression near the wound site at early regeneration stages, potentially indicating the importance of riboflavin for wound healing (Figure 6). This is supported by a study that found that RF deficiency slowed the rate of skin wound contraction in rats (55). Together, these findings indicate that RF transport is potentially important for stem cell dynamics during planarian regeneration, supported by the fact that RFT deficiency is associated with impaired mitochondrial function and redox imbalance, which negatively impacts stem cell function (25, 56, 57). Moreover, it has been shown that RF transporters are overexpressed in many tumour types, including squamous cell carcinoma, melanoma, and luminal A breast cancer, likely due to the high metabolic demands of cancer cells. Additionally, it was demonstrated that cancer cells exhibit increased RF metabolism compared to normal cells (58). Given the striking parallels between cancer cells and stem cells, regarding their self-renewal capacity and the use of similar signalling pathways, this high demand for RF in cancer cells suggests the possibility that RFK and RFT, responsible for proper availability of RF and its derivatives, is also crucial for stem cell function (59). To study whether the early *Smed-RFT* expression at the wound site is

potentially an upregulation, a spatio-temporal characterization of RFT should be performed involving various time points, including 0hpa.

In addition to investigating whether RF may be an important component and modulator of the AOX system, we also explored how the AOX response is regulated. Therefore, we studied the role of the evolutionary conserved redox-regulating Keap1/Nrf2 signalling pathway during regeneration in *S. mediterranea*. However, an examination of PlanMine (v3.0) data indicated that the transcription factor Nrf2 is not expressed in *S. mediterranea*. Although this observation initially suggested that the classical Nrf2 pathway might not be operational in these organisms, further analysis revealed that Keap1, a critical regulator of Nrf2, is indeed expressed in the planarian. Given the functional homology of SKN-1 to the mammalian Nrf2 in *C. elegans*, we examined and confirmed the presence of SKN-1 in *S. mediterranea*. SKN-1 in *C. elegans* has been shown to play a crucial role in oxidative stress response and longevity, similar to Nrf2 in mammals (40).

Having confirmed the expression of both *Smed-Keap1* and *Smed-SKN-1* in planarians, our study sought to unveil their functional roles in regulating the AOX response during planarian regeneration by silencing the *Smed-Keap1* and *Smed-SKN-1* related targets via RNAi. The experimental results indicate that silencing the targeted genes does not significantly impact the formation of new tissue or the development of photoreceptors (Figure 7b,d). This observation suggests the presence of compensatory mechanisms that mitigate the effects of gene knockdown, thereby preserving normal regenerative processes. One plausible compensatory mechanism could involve RF, which is known to play a critical role in cellular metabolism and oxidative stress response (33, 36). As an important molecule with antioxidative properties, RF might have the potential to rescue regeneration after silencing *Smed-Keap1* or *Smed-SKN-1*. Bijnens and colleagues underscored the importance of antioxidants in mitigating oxidative stress for successful planarian regeneration as inhibition of approximately 60% of SOD activity resulted in the regeneration of severe phenotypes (30). Given that our intervention targeted specific proteins associated with the AOX system individually rather than the entire AOX system, it is plausible that other components of this system, such as RF, GSH, or CAT, compensate and rescue regeneration. A study by Bjelakovic *et al* that indicated that altering the levels of one antioxidant causes compensatory changes in the levels of other antioxidants, while the overall AOX capacity remains unchanged (60). However, this warrants further investigation. To study neurodevelopment after *Smed-Keap1* or *Smed-SKN-1* knockdown, the planarians' cognitive function was assessed. The results concerning the planarians' cognitive performance were somewhat variable (Figure 7c). Given that the *Smed-Keap1* and *Smed-SKN1_2* transcripts are expressed in neuronal cell types, a role in neurodevelopment is plausible, supported by the PC2 and TH stainings, revealing a smaller brain, following *Smed-Keap1_2* knockdown (Supplemental Figure 2). However, on the one hand knockdown of *Smed-Keap1_2* impairs motility and increased light avoidance capacity of the treated tails and on the other hand knockdown of *Smed-SKN1_2* improves motility and does not significantly affect light avoidance capacity. Considering the inconsistencies in cognitive function results, it is suggested to repeat the experiment including a larger sample size. The diverse expression patterns of *Smed-Keap1* and *Smed-SKN-1* transcripts suggest that each plays distinct roles in different cell types, impacting motility and sensory behaviours in others ways (Figure 7e). Considering that, in the absence of stress stimuli, Keap1 binds Nrf2 and prevents its translocation to the nucleus to orchestrate an AOX response, the observed lack of effects on tissue regeneration and photoreceptor development could potentially be attributed to the absence of oxidative stress in the experimental conditions (61).

Using the pharmacological inhibitor DETC to induce oxidative stress by reducing SOD activity allowed us to study the functional roles of *Smed-Keap1* and *Smed-SKN-1* during regeneration in relation to their redox-regulating capacity. A notable observation was the presence of a stress phenotype following DETC exposure, even in the control group (Figure 8b). This result might be solely attributed to the effects of DETC, as demonstrated in a study by Bijnens and colleagues, which found that DETC exposure, inhibiting approximately 60% of SOD activity, causes a more severe phenotype than RNAi-mediated interference with SOD levels (30). However, our results also revealed that DETC alone did not significantly affect blastema formation and eye development, probably because DETC exposure without interference

with other antioxidant genes allows for compensatory mechanisms to rescue the regeneration process (Figure 8b,c,d). However, the combination of DETC exposure and *Smed-Keap1* knockdown reduced blastema size and impaired eye development at 7 dpa, in addition to causing blister formation (Figure 8c,d). This suggests that *Smed-Keap1* knockdown in a situation of oxidative stress can override compensatory mechanisms other than SOD, as evidenced by the lack of rescue in regeneration. A study by Hu and colleagues investigated the modulating effect of Keap1 on the cell cycle of replicating hepatocytes during liver regeneration in mice. They revealed that Keap1 knockdown caused a severe disruption in both the redox cycle and the cell cycle of replicating hepatocytes in addition to dysregulation of Nrf2 activity during liver regeneration, highlighting the importance of Keap1 as a redox-regulating compound during regeneration (62). The combination of *Smed-SKN-1* knockdown and DETC exposure also impaired blastema formation and photoreceptor development to some extent, but these effects were less pronounced compared to those following *Smed-Keap1* knockdown (Figure 9c,d). In *C. elegans*, SKN-1 orchestrates an AOX response by activating the expression of genes involved in oxidative stress defence, possibly similar to its role in planarians as suggested by the results (63). These findings indicate that compensatory mechanisms are less effective in rescuing regeneration when *Smed-Keap1* or *Smed-SKN-1* are compromised, highlighting the importance of these genes in regulating the AOX response. Further investigation is necessary to elucidate how *Smed-Keap1* and *Smed-SKN-1* exactly function during planarian regeneration.

CONCLUSION

This exploratory study delved deeper into the complex process of redox-mediated regeneration in *S. mediterranea*, with a focus towards the redox-sensitive vitamin, RF, and the redox-regulating proteins, Keap1 and SKN-1. In conclusion, our research was successful in providing evidence for the significant role of RF in various aspects of planarian regeneration. Our findings suggest that RF transport is expressed close to the wound site during the early stages of regeneration, implicating its importance in facilitating RF availability for successful wound healing. Moreover, our results indicate a potential role of RF in promoting stem cell proliferation, highlighting its involvement in the regenerative processes crucial for tissue repair. Additionally, our study suggests that RF metabolism plays an important role in tissue regeneration, photoreceptor development and dopaminergic neuron development. Furthermore, our study reveals the expression of *Smed-Keap1* and *Smed-SKN-1* in *S. mediterranea* with a redox-regulating role during regeneration. Collectively, these findings address research gaps in the current understanding of the process of redox-mediated planarian regeneration and potentially offer valuable insights into biological processes relevant to the advancement of regenerative medicine.

Acknowledgements – I would like to extend my deepest gratitude to my supervisor, Martijn Heleven and promotor, Karen Smeets, for their guidance and support throughout this research project. Their expertise, insights, and constructive feedback were crucial to the completion of this project and greatly improved the quality of this work. I am also grateful to the members of the BiTElab research group at Hasselt University for the pleasant lab experience. I am appreciative of Martijn Heleven for his training, technical support and assistance with confocal microscopy. On a personal note, I wish to express my heartfelt thanks to friends and family for their unwavering moral support and encouragement throughout this journey. Finally, a special thanks to my supervisor, Martijn Heleven, whose guidance has been pivotal in my academic growth.

Author contributions – Karen Smeets and Martijn Heleven conceived and designed the project. Renée Moonen conducted the experiments and performed data analysis. Renée Moonen wrote the manuscript with significant input from Martijn Heleven.

REFERENCES

1. Pirotte N, Stevens AS, Fraguas S, Plusquin M, Van Roten A, Van Belleghem F, et al. Reactive Oxygen Species in Planarian Regeneration: An Upstream Necessity for Correct Patterning and Brain Formation. Oxid Med Cell Longev. 2015;2015:392476.
2. Elchaninov AV, Sukhikh GT, Fatkhudinov TK, editors. Evolution of Regeneration in Animals: A Tangled Story. Frontiers in Ecology and Evolution; 2021.
3. Jaenen V, Fraguas S, Bijnens K, Heleven M, Artois T, Romero R, et al. Reactive oxygen species rescue regeneration after silencing the MAPK-ERK signaling pathway in Schmidtea mediterranea. Sci Rep. 2021;11(1):881.
4. Fumagalli MR, Zapperi S, La Porta CAM. Regeneration in distantly related species: common strategies and pathways. NPJ Syst Biol Appl. 2018;4:5.
5. Gurtner GC, Werner S, Barrandon Y, Longaker MT. Wound repair and regeneration. Nature. 2008;453(7193):314-21.
6. Dall'Agnese A, Puri PL. Could we also be regenerative superheroes, like salamanders? Bioessays. 2016;38(9):917-26.
7. Byrne M, Mazzone F, Elphick MR, Thorndyke MC, Cisternas P. Expression of the neuropeptide SALMFamide-1 during regeneration of the seastar radial nerve cord following arm autotomy. Proc Biol Sci. 2019;286(1901):20182701.
8. Poss KD, Wilson LG, Keating MT. Heart regeneration in zebrafish. Science. 2002;298(5601):2188-90.
9. Hickman D. Commonly Used Animal Models. . 2017.
10. Reddien PW. The Cellular and Molecular Basis for Planarian Regeneration. Cell. 2018;175(2):327-45.
11. Goel T, Ireland D, Shetty V, Rabeler C, Diamond PH, Collins ES. Let it rip: the mechanics of self-bisection in asexual planarians determines their population reproductive strategies. Phys Biol. 2021;19(1).
12. King RS, Newmark PA. The cell biology of regeneration. J Cell Biol. 2012;196(5):553-62.
13. Liu Y, Lou WP, Fei JF. The engine initiating tissue regeneration: does a common mechanism exist during evolution? Cell Regen. 2021;10(1):12.
14. Sasidharan V, Lu YC, Bansal D, Dasari P, Poduval D, Seshasayee A, et al. Identification of neoblast- and regeneration-specific miRNAs in the planarian Schmidtea mediterranea. Rna. 2013;19(10):1394-404.
15. Romito A, Cobellis G. Pluripotent Stem Cells: Current Understanding and Future Directions. Stem Cells Int. 2016;2016:9451492.
16. Wen X, Jiao L, Tan H. MAPK/ERK Pathway as a Central Regulator in Vertebrate Organ Regeneration. Int J Mol Sci. 2022;23(3).
17. Abdal Dayem A, Hossain MK, Lee SB, Kim K, Saha SK, Yang GM, et al. The Role of Reactive Oxygen Species (ROS) in the Biological Activities of Metallic Nanoparticles. Int J Mol Sci. 2017;18(1).
18. Ray PD, Huang BW, Tsuji Y. Reactive oxygen species (ROS) homeostasis and redox regulation in cellular signaling. Cell Signal. 2012;24(5):981-90.
19. Tirichen H, Yaigoub H, Xu W, Wu C, Li R, Li Y. Mitochondrial Reactive Oxygen Species and Their Contribution in Chronic Kidney Disease Progression Through Oxidative Stress. Front Physiol. 2021;12:627837.
20. Checa J, Aran JM. Reactive Oxygen Species: Drivers of Physiological and Pathological Processes. J Inflamm Res. 2020;13:1057-73.
21. Love NR, Chen Y, Ishibashi S, Kritsiligkou P, Lea R, Koh Y, et al. Amputation-induced reactive oxygen species are required for successful Xenopus tadpole tail regeneration. Nat Cell Biol. 2013;15(2):222-8.
22. Gauron C, Rampon C, Bouzaffour M, Ipendey E, Teillon J, Volovitch M, et al. Sustained production of ROS triggers compensatory proliferation and is required for regeneration to proceed. Sci Rep. 2013;3:2084.
23. Vogg MC, Buzgariu W, Suknovic NS, Galliot B. Cellular, Metabolic, and Developmental Dimensions of Whole-Body Regeneration in Hydra. Cold Spring Harb Perspect Biol. 2021;13(12).
24. Ivankovic M, Haneckova R, Thommen A, Grohme MA, Vila-Farré M, Werner S, et al. Model systems for regeneration: planarians. Development. 2019;146(17).

25. Wang K, Zhang T, Dong Q, Nice EC, Huang C, Wei Y. Redox homeostasis: the linchpin in stem cell self-renewal and differentiation. Cell Death Dis. 2013;4(3):e537.
26. Singh A, Kukreti R, Saso L, Kukreti S. Oxidative Stress: A Key Modulator in Neurodegenerative Diseases. Molecules. 2019;24(8).
27. Sharma P. Reactive Oxygen Species, Oxidative Damage, and Antioxidative Defense Mechanism in Plants under Stressful Conditions. . Journal of Botany. 2011.
28. Wang Y, Branicky R, Noë A, Hekimi S. Superoxide dismutases: Dual roles in controlling ROS damage and regulating ROS signaling. J Cell Biol. 2018;217(6):1915-28.
29. Marí M, Morales A, Colell A, García-Ruiz C, Fernández-Checa JC. Mitochondrial glutathione, a key survival antioxidant. Antioxid Redox Signal. 2009;11(11):2685-700.
30. Bijnens K, Jaenen V, Wouters A, Leynen N, Pirotte N, Artois T, et al. A Spatiotemporal Characterisation of Redox Molecules in Planarians, with a Focus on the Role of Glutathione during Regeneration. Biomolecules. 2021;11(5).
31. Rosa MT, Weiblen AM, Oliveira MDD, Almeida BFA, Pavão LH, Waczuk MP, et al. Aloe Extracts, Pro and Antioxidant Conditions in Regeneration of the Planarian Girardia tigrina. Journal of Biologically Active Products from Nature. 2017;7:278-93.
32. Tsarkova E, Filippova K, Afanasyeva V, Ermakova O, Kolotova A, Blagodatski A, et al. A Study on the Planarian Model Confirms the Antioxidant Properties of Tameron against X-ray- and Menadione-Induced Oxidative Stress. Antioxidants (Basel). 2023;12(4).
33. Suwannasom N, Kao I, Pruß A, Georgieva R, Bäumler H. Riboflavin: The Health Benefits of a Forgotten Natural Vitamin. Int J Mol Sci. 2020;21(3).
34. Peechakara BV, Sina RE, Gupta M. Vitamin B2 (Riboflavin). StatPearls. Treasure Island (FL): StatPearls Publishing
Copyright © 2024, StatPearls Publishing LLC.; 2024.
35. Sinha T, Naash MI, Al-Ubaidi MR. Flavins Act as a Critical Liaison Between Metabolic Homeostasis and Oxidative Stress in the Retina. Front Cell Dev Biol. 2020;8:861.
36. Olfat N, Ashoori M, Saedisomeolia A. Riboflavin is an antioxidant: a review update. Br J Nutr. 2022;128(10):1887-95.
37. Baird L, Yamamoto M. The Molecular Mechanisms Regulating the KEAP1-NRF2 Pathway. Mol Cell Biol. 2020;40(13).
38. Velichkova M, Hasson T. Keap1 regulates the oxidation-sensitive shuttling of Nrf2 into and out of the nucleus via a Crm1-dependent nuclear export mechanism. Mol Cell Biol. 2005;25(11):4501-13.
39. Ngo V, Duennwald ML. Nrf2 and Oxidative Stress: A General Overview of Mechanisms and Implications in Human Disease. Antioxidants (Basel). 2022;11(12).
40. Tullet JMA, Green JW, Au C, Benedetto A, Thompson MA, Clark E, et al. The SKN-1/Nrf2 transcription factor can protect against oxidative stress and increase lifespan in C. elegans by distinct mechanisms. Aging Cell. 2017;16(5):1191-4.
41. Wilson MA, Iser WB, Son TG, Logie A, Cabral-Costa JV, Mattson MP, et al. skn-1 is required for interneuron sensory integration and foraging behavior in Caenorhabditis elegans. PLoS One. 2017;12(5):e0176798.
42. King RS, Newmark PA. In situ hybridization protocol for enhanced detection of gene expression in the planarian Schmidtea mediterranea. BMC Dev Biol. 2013;13:8.
43. Plusquin M, Stevens AS, Van Belleghem F, Degheselle O, Van Roten A, Vroonen J, et al. Physiological and molecular characterisation of cadmium stress in Schmidtea mediterranea. Int J Dev Biol. 2012;56(1-3):183-91.
44. Rozanski A, Moon H, Brandl H, Martín-Durán JM, Grohme MA, Hüttner K, et al. PlanMine 3.0-improvements to a mineable resource of flatworm biology and biodiversity. Nucleic Acids Res. 2019;47(D1):D812-d20.
45. Liu H, Du Y, St-Pierre JP, Bergholt MS, Autefage H, Wang J, et al. Bioenergetic-active materials enhance tissue regeneration by modulating cellular metabolic state. Sci Adv. 2020;6(13):eaay7608.
46. Wang YP, Wei JY, Yang JJ, Gao WN, Wu JQ, Guo CJ. Riboflavin supplementation improves energy metabolism in mice exposed to acute hypoxia. Physiol Res. 2014;63(3):341-50.
47. Mazzotta C, Caragiuli S, Caporossi A. Riboflavin and the Cornea and Implications for Cataracts. 2014. p. 123-30.

48. Sinha T, Ikelle L, Makia MS, Crane R, Zhao X, Kakakhel M, et al. Riboflavin deficiency leads to irreversible cellular changes in the RPE and disrupts retinal function through alterations in cellular metabolic homeostasis. Redox Biol. 2022;54:102375.
49. Koziol B, Markowicz M, Kruk J, Plytycz B. Riboflavin as a source of autofluorescence in Eisenia fetida coelomocytes. Photochem Photobiol. 2006;82(2):570-3.
50. Boulton AA, Eisenhofer G. Catecholamine metabolism. From molecular understanding to clinical diagnosis and treatment. Overview. Adv Pharmacol. 1998;42:273-92.
51. Prah A, Purg M, Stare J, Vianello R, Mavri J. How Monoamine Oxidase A Decomposes Serotonin: An Empirical Valence Bond Simulation of the Reactive Step. J Phys Chem B. 2020;124(38):8259-65.
52. Sarkar A, Mukundan N, Sowndarya S, Dubey VK, Babu R, Lakshmanan V, et al. Serotonin is essential for eye regeneration in planaria Schmidtea mediterranea. FEBS Lett. 2019;593(22):3198-209.
53. Fennessy JR, Cornett KMD, Burns J, Menezes MP. Benefit of high-dose oral riboflavin therapy in riboflavin transporter deficiency. J Peripher Nerv Syst. 2023;28(3):308-16.
54. Plazaola-Sasieta H, Zhu Q, Gaitán-Peñas H, Rios M, Estévez R, Morey M. Drosophila ClC-a is required in glia of the stem cell niche for proper neurogenesis and wiring of neural circuits. Glia. 2019;67(12):2374-98.
55. Lakshmi R, Lakshmi AV, Bamji MS. Skin wound healing in riboflavin deficiency. Biochem Med Metab Biol. 1989;42(3):185-91.
56. Colasuonno F, Niceforo A, Marioli C, Fracassi A, Stregapede F, Massey K, et al. Mitochondrial and Peroxisomal Alterations Contribute to Energy Dysmetabolism in Riboflavin Transporter Deficiency. Oxid Med Cell Longev. 2020;2020:6821247.
57. Zhang H, Menzies KJ, Auwerx J. The role of mitochondria in stem cell fate and aging. Development. 2018;145(8).
58. Darguzyte M, Drude N, Lammers T, Kiessling F. Riboflavin-Targeted Drug Delivery. Cancers (Basel). 2020;12(2).
59. Reya T, Morrison SJ, Clarke MF, Weissman IL. Stem cells, cancer, and cancer stem cells. Nature. 2001;414(6859):105-11.
60. Bjelakovic G, Nikolova D, Gluud LL, Simonetti RG, Gluud C. Antioxidant supplements for prevention of mortality in healthy participants and patients with various diseases. Cochrane Database Syst Rev. 2012;2012(3):Cd007176.
61. Kobayashi A, Kang MI, Okawa H, Ohtsuji M, Zenke Y, Chiba T, et al. Oxidative stress sensor Keap1 functions as an adaptor for Cul3-based E3 ligase to regulate proteasomal degradation of Nrf2. Mol Cell Biol. 2004;24(16):7130-9.
62. Hu M, Zou Y, Nambiar SM, Lee J, Yang Y, Dai G. Keap1 modulates the redox cycle and hepatocyte cell cycle in regenerating liver. Cell Cycle. 2014;13(15):2349-58.
63. An JH, Vranas K, Lucke M, Inoue H, Hisamoto N, Matsumoto K, et al. Regulation of the Caenorhabditis elegans oxidative stress defense protein SKN-1 by glycogen synthase kinase-3. Proceedings of the National Academy of Sciences. 2005;102(45):16275-80.

SUPPLEMENTARY

Supplemental Experimental Procedures

FISH protocol - On the first day, mucus was removed using 7.5% N-Acetyl-L-cysteine (NAC) in phosphate-buffered saline (PBS), after which planarians were fixed in 4% formaldehyde (FA) in PBSTx (PBS + 0.3% Triton X-100) to preserve tissues, and dehydrated in a methanol series for storage at -20°C. On the second day, fixed planarians were rehydrated and bleached in 6% formamide for 2h to remove pigmentation. Subsequently, bleached planarians were permeabilized with proteinase K, followed by hybridization with fluorescently labelled RNA probes (diluted 1:300). The third day involved post-hybridization washes with saline-sodium citrate (SCC) buffer to remove unbound probes, blocking of non-specific binding sites, and incubation with Anti-digoxigenin peroxidase (Anti-dig POD, Sigma-Aldrich, diluted 1:2000) antibodies. On the final day, excess antibodies were washed off with Tris-NaCl-Tween (TNT) buffer and a Tyramide Signal Amplification (TSA) reaction was performed. Following mounting in ImmuMount (Thermo Fisher Scientific, Waltham, MA, USA), images were captured using a Zeiss LSM900 confocal microscope.

Smedwi-1 immunohistochemistry - For the co-localization with stem cells, we employed a combined FISH and immunostaining protocol. On the fourth day of the FISH protocol, more specifically after the TSA reaction, an immunostaining for the general stem cell marker, *Smedwi-1*, was conducted. On the first day, samples were blocked in 1% bovine serum albumin (BSA) for 2h at room temperature (RT) and incubated with primary anti-Smedwi-1 (diluted 1:1000 in 1% BSA/PBSTx) antibody overnight (ON) at 4°C. The following day, samples were washed with PBSTx, blocked again with 1% BSA/PBSTx for 2h at RT, and incubated with the secondary goat anti-rabbit-IgG Alexa Fluor 568-conjugated antibody (Thermo Fisher Scientific, Cat. No. A-11036, diluted 1:500 in 1% BSA/PBSTx) ON at 4°C or for 3h at RT. Following final washing steps in PBST and mounting in ImmuMount (Thermo Fisher Scientific), images were captured using a Zeiss LSM900 confocal microscope, and fluorescence intensity measurements were subsequently determined. The mean intensity of fluorescence was determined using the Zeiss LSM900 confocal microscope and normalised against the mean body size that was determined using ImageJ software (v2.3.1).

Anti-SYNORF-1 immunohistochemistry - Differences in regeneration of the CNS were examined by performing an immunostaining using anti-SYNORF-1, a mouse monoclonal antibody specific for synapsin (3C11, Developmental Studies Hybridoma Bank, Iowa, IA, USA, diluted 1:50 in 1% BSA/PBSTx). Regenerating animals were killed by immersion in 2% HCl and then fixed in 4% FA/PBSTx. After fixation, animals were processed as described in (1). The secondary goat anti-mouse Alexa Fluor 488-conjugated antibody (Molecular Probes,, diluted 1:400) was used. Following mounting in ImmuMount (Thermo Fisher Scientific), images were captured using a Zeiss LSM900 confocal microscope. Relative brain ganglia widths were determined by normalizing brain width against head width (Supplemental Figure 1). Image analysis was conducted using ImageJ software (v2.3.1) on digital images.

Supplemental Table

Table 1: Overview of primer sequences.

Target	Transcript	Forward primer	Reverse primer	Forward-T7 primer	Reverse-T7 primer
Smed-RFK	dd_Smed_v6_1500_0_1	gcggggaagtaaagaattgg	atgatttccgcttgttctgg	GGATCCTAATACGACTCACTATA GGGgcggggaagtaaagaattgg	GGATCCTAATACGACTCACTATA GGGatgatttccgcttgttctgg
Smed-RFT	dd_Smed_v6_5546_0_1	gtgttggaggtgaaggacgt	agccaaacgtgaccctgtt	GGATCCTAATACGACTCACTATA GGGgtgttggaggtgaaggacgt	GGATCCTAATACGACTCACTATA GGGagccaaacgtgaccctgtt
Smed-Keap1_1	dd_Smed_v6_1751_0_1	tgttcagttcacggtcgagtt	accgcatgtccagattttcca	GGATCCTAATACGACTCACTATA GGGtgttcagttcacggtcgagtt	GGATCCTAATACGACTCACTATA GGGaccgcatgtccagattttcca
Smed-Keap1_2	dd_Smed_v6_1751_0_1	caaacgtgtgctccaatgtct	agccaccaaacacccaaatt	GGATCCTAATACGACTCACTATA GGGcaaacgtgtgctccaatgtct	GGATCCTAATACGACTCACTATA GGGagccaccaaacacccaaatt
Smed-SKN1_1	dd_Smed_v6_4539_0_1	ctgatgactgtagcccaacga	cccgaatggtgctgtgaattc	GGATCCTAATACGACTCACTATA GGGctgatgactgtagcccaacga	GGATCCTAATACGACTCACTATA GGGcccgaatggtgctgtgaattc
Smed-SKN1_2	dd_Smed_v6_1864_0_1	gagctggtctgatgagtattt	aaattttcctgtgtgcattagaa	GGATCCTAATACGACTCACTATA GGGgagctggtctgatgagtattt	GGATCCTAATACGACTCACTATA GGGaaattttcctgtgtgcattagaa
Smed-SKN1_3	dd_Smed_v6_10446_0_1	tcagagatcaagcgactccaa	agtgtagaaggcatagtcgaatct	GGATCCTAATACGACTCACTATA GGGtcagagatcaagcgactccaa	GGATCCTAATACGACTCACTATA GGGagtgtagaaggcatagtcgaatct

Supplemental Figures

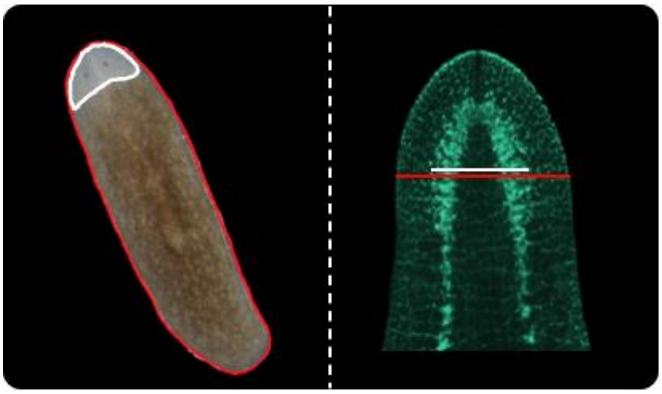

Supplemental Figure S1: Methods for blastema (left) and ganglia development (right) measurements. Regenerating tail at 7 dpa as an example for blastema measurements on the left; blastema size (white) was normalised against the total body area (red). Cephalic ganglia at 7 dpa as an example for ganglia measurements; brain ganglia width (white) was normalised against head width (red). Abbreviations: *dpa, days post amputation*.

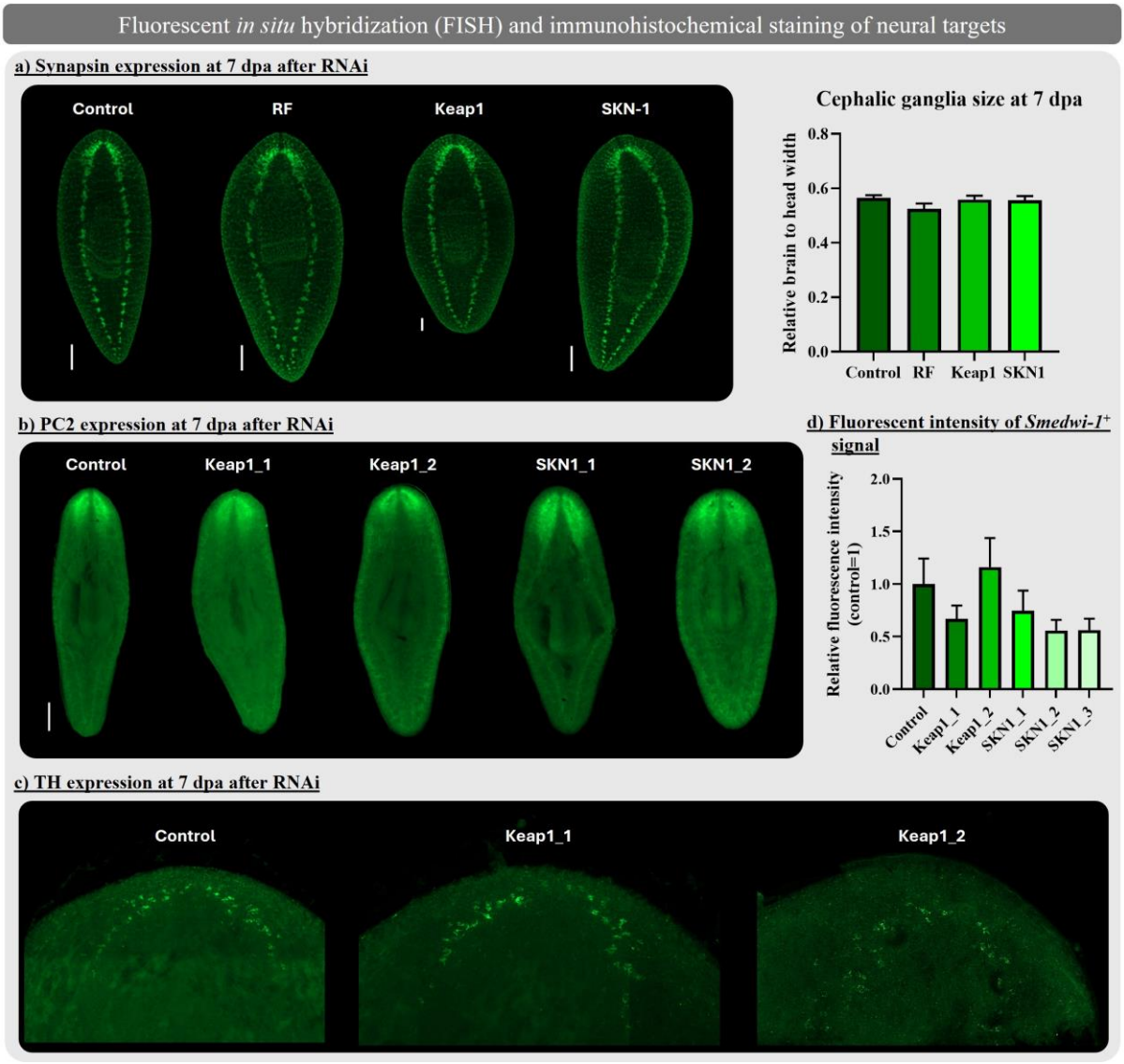

Supplementary Figure S2: Expression patterns neuronal markers following RNAi treatment. **a)** Following knockdown of RF-related targets (*Smed-RFK* and *Smed-RFT*), *Smed-Keap1*, and *Smed-SKN-1* related targets, planarians were fixed and stained for anti-synapsin (green, 488nm), a marker of the central nervous system (CNS), using FISH at 7 dpa. Scale bars of 200 µm and 100 µm (Keap1). The bar graph depicts the relative brain to head width as a measure of cephalic ganglia (brain) size. **b)** Following knockdown of *Smed-Keap1* and *Smed-SKN-1* related targets, planarians were fixed and stained for prohormone convertase 2 (PC2) (green, 488nm) using FISH at 7 dpa. Scale bar of 200 µm. **c)** Following knockdown of *Smed-Keap1* and *Smed-SKN-1* related targets, planarians were fixed and stained for tyrosine hydroxylase (TH) (green, 488nm) using FISH at 7 dpa. Images were magnified to show expression within the cephalic ganglia. **d)** The aforementioned stainings for TH, PC2, and synapsin were co-localised with stem cells using an immunolabelling for the general stem cell marker *Smedwi-1*. The *Smedwi-1* fluorescent signal was then measured. The bar graph depicts the average intensity of the *Smedwi-1*$^{+}$ signal per condition normalised against the control. Abbreviations: *RNAi, RNA interference; RF, riboflavin; RFK, riboflavin kinase; RFT, riboflavin transporter; Keap1, Kelch-like ECH-associated protein 1; SKN-1, Skinhead-1; dpa, days post amputation; nm, nanometer; µm, micrometer*.